NASA CR-72644
Stellite 70-7691

Superalloy by Powder Metallurgy for use at 1000 - 1400°F

by

P.S. Kotval

UNION CARBIDE CORPORATION
MATERIALS SYSTEMS DIVISION

prepared for

NATIONAL AERONAUTICS AND SPACE ADMINISTRATION

NASA LEWIS RESEARCH CENTER
CONTRACT NAS 3-13214
FREDRIC H. HARF, PROJECT MANAGER

Submitted
December 31, 1969
NASA CR-72644

FINAL REPORT

SUPERALLOY BY POWDER METALLURGY FOR USE AT 1000-1400°F

by

P. S. Kotval

UNION CARBIDE CORPORATION
MATERIALS SYSTEMS DIVISION
P. O. Box 24184
Indianapolis, Indiana 46224

prepared for

NATIONAL AERONANUTICS AND SPACE ADMINISTRATION
CONTRACT NAS 3-13214

NASA Lewis Research Center
Fredric H. Harf, Project Manager
Materials and Structures Division

FOREWORD

The work described herein was performed at Materials Systems Division, Union Carbide Corporation under NASA Contract NAS-3 13214 with Mr. Fredric H. Harf as NASA Project Manager. The work was performed both at the Speedway and Kokomo Laboratories of Materials Systems Division. The author and the latter facility is now a part of the Stellite Division of Cabot Corporation. The author of this report would like to acknowledge the following colleagues whose assistance and advice allowed rapid progress to be made in the completion of this study - Messrs. J. S. Dickey, G. W. Gordon, T. A. Turner, J. W. Shutt and T. Jones.

TABLE OF CONTENTS

LIST OF TABLES

LIST OF ILLUSTRATIONS

LIST OF ILLUSTRATIONS - Continued

ABSTRACT

Argon atomized nickel-base alloy powders of two compositions were consolidated by extrusion and processed thermomechanically. The compositions are strengthened by precipitation of the body-centered-tetragonal Ni_3Ta or Ni_3Cb phases. Microstructural observations indicated good stability for the Ni_3Ta phase up to 1400°F (760°C). Mechanical property measurements showed a tensile yield strength of 189,000 psi (1300 N/mm^2) at 1200°F (650°C) for the alloy strengthened by the Ni_3Ta phase with greater than 10 percent elongation.

SUMMARY

This work was undertaken with the objective of ascertaining the feasibility of producing a high-strength 1000-1400°F powder-metallurgy alloy in which precipitation of a tetragonal coherent γ'' phase would be the principal strengthening mechanism. Two compositions were evaluated in which the coherent body-centered-tetragonal γ'' phases were Ni_3Ta and Ni_3Cb, respectively.

Alloy 1 - Ni - 20 Cr - 10 Co - 7.0 Mo - 9.5 Ta - .05 C - .02 Oxygen

Alloy 2 - Ni - 20 Cr - 10 Co - 7.0 Mo - 7.0 Cb - .05 C - .02 Oxygen

Argon atomized powder of these two compositions was consolidated by canning and hot extrusion. Subsequently, the extruded material was cold-worked and aged to precipitate the body-centered-tetragonal γ'' phase in either case. (Ni_3Ta in Alloy 1 and Ni_3Cb in Alloy 2). Extensive microstructural analysis, involving optical microscopy, scanning and transmission electron microscopy (both thin foils and replicas) and diffraction, was performed in this study.

In addition, a limited program of evaluation of mechanical properties was carried out. Of the two systems investigated, in Alloy 1 a Ni_3Ta strengthened powder-metallurgy alloy system has been defined in which the 1200°F (650°C) tensile yield strength is 189,000 psi (1300 MN/m^2) with greater than 10 percent ductility and the stress-rupture life at 110,000 psi (755 MN/m^2) and 1200°F (650°C) is of the order of 40 hours. After 100 hours exposure at 1400°F (760°C), 92 percent of the above yield strength is retained at 1200°F (650°C).

In this work no attempt has been made at optimizing the thermomechanical treatments to obtain the highest tensile and stress rupture properties. The results, however, show feasibility and point to the potential of strengthening a powder metallurgy superalloy by precipitation of the body-centered-tetragonal γ'' phase.

INTRODUCTION

The powder metallurgy processing method to produce fully-dense consolidated material has been applied to several superalloy compositions over the last 5 to 10 years. Work[1,2,3] on pre-alloyed powders of B-1900, IN-100, 713-C type compositions has shown the feasibility of consolidating such powders. However, most of these attempts have concentrated on the powder-processing technique using existent commercial alloy compositions and subsequent property evaluation of the consolidated material.

The present work was undertaken to ascertain the feasibility of utilizing the powder-processing method using certain previously-developed, precipitation-strengthenable superalloy compositions to produce a high-strength superalloy bar for 1000-1400°F (540-760°C) applications.

For the present program, powders were prepared by inert gas atomization of a pre-alloyed master melt. After screening and separation, powders were canned in steel jackets under argon and extruded at a ratio of 8.2 to 1 to provide 19.0 mm. diameter bar. This as-consolidated material has been processed by cold-swaging and subsequent aging. Mechanical properties have been evaluated for this precipitation-strengthened material and structural observations have been carried out using optical, replica and thin foil transmission metallographic techniques.

The data reported herein includes extensive microstructural observations on both the as-atomized powders and as-consolidated material in various stages of thermomechanical treatment for two experimental alloy compositions. The feasibility studies have excluded any attempt at optimizing thermomechanical processing or heat treatments; nevertheless, the processing sequence and heat-treatments chosen for this study have shown that a high strength P/M alloy system has been defined which relies upon the precipitation of a body-centered-tetragonal Ni_3M phase for its strength. Of the two P/M alloy systems investigated, Alloy 1 is a Ni_3Ta strengthened system. At 1200°F (650°C), this system has manifested a tensile yield strength of 189,000 psi (1296 MN/m^2) with better than 10 percent elongation. After a 100 hour exposure at 1400°F (760°C), 92 percent of these 1200°F (650°C) strength levels are retained. In stress-rupture tests at 1200°F (650°C) the material shows properties comparable to the wrought superalloys currently in use.

EXPERIMENTAL PROCEDURES AND RESULTS

Alloy Preparation

140 pound (63 kg.) heats of two alloys were vacuum induction melted. The nominal compositions sought were (in weight percent):

Alloy 1 - Ni-20Cr-9.5Co-7.0Mo-9.5Ta-0.05C-<0.02 Oxygen

Alloy 2 - Ni-20Cr-9.5Co-7.0Mo-7.0Cb-0.05C-<0.020 Oxygen

In each case the material was cast into remelt bars. These bars were remelted in a small induction furnace and atomized in a horizontal argon-filled tank. The atomization process involved the impingement of a high pressure argon gas stream upon the stream of molten metal emanating from a specially designed nozzle. The interaction of the high pressure gas on the molten stream causes "atomization" to occur. The droplets of as-atomized material are rapidly solidified by contact with the inert gas within the horizontal cylinder chamber and collect therein. Various distributions of sizes are possible in this process dependent upon the atomization parameters; nozzle temperature, degree of superheat and inert gas pressure being the primary controlling factors. In the present investigation a liquid metal temperature of 2950°F (1620°C) and argon pressure of 350 psi (2.40 MN/m^2) was used in the atomization process. These conditions were chosen to minimize the oxygen content of the resultant powders and as a necessary consequence the coarse particle fraction of the as-atomized powders was higher than normal. The "clean-up" weight, i.e., the weight of all atomized material collected from the atomization chamber was 98 pounds (44.6 kg.) for Alloy 1 and 105 pounds (47.8 kg.) for Alloy 2.*

As-atomized powders were screened under argon to separate the -100 mesh fraction and further screened to separate out the -325 mesh fraction and to retain the -100/+325 mesh fraction. (At this point, microstructural work on as-atomized powders was carried out as reported later in the text.) The overall weight of the -100 fraction for Alloy 1 was 48 pounds (22.0 kg.) and for Alloy 2, 52 pounds (24.0 kg.). Oxygen analyses were carried out on each alloy for both the -100 and the -100/+325 mesh fraction using a neutron activation analysis technique. The oxygen levels were found to be as follows:

TABLE I

Oxygen Analyses

	Alloy 1	Alloy 2
-100/+325 Fraction	163 ppm 159 ppm	73 ppm 68 ppm
-100 Down Fraction	189 ppm	159 ppm 118 ppm

* Difficulty was experienced in maintaining adequately low oxygen levels for Alloy 2 and three heats had to be atomized before an acceptable composition was obtained. It is the acceptable final heat that is reported here.

The -325 mesh fraction of the -100 mesh material was, respectively, 13 pounds (6.0 kg.) out of 48 pounds (21.8 kg.) for Alloy 1 and 15 pounds (6.8 kg.) out of 52 pounds (23.6 kg.) for Alloy 2. Thus it was clear that exclusion of the -325 mesh fraction from subsequent processing would reduce the amount of available material but also permit lower O_2 levels (per the above quoted analysis) in the eventually consolidated material. Accordingly, -100/+325 mesh blended powder was divided into approximately 2.5 pounds (1.14 kg.) batches and canned in a 63.5 mm. O.D. cylindrical steel jacket with 6.35 mm. wall thickness which was closed at either end. The front end of the steel can comprised a 45° tapered conical frustrum and the back-end comprised a plate with an evacuation aperture. After welding of the end-plate the can and contents were evacuated, back-filled with argon and the evacuation aperture then sealed.

Extrusion of the powder-filled can was carried out at 2200°F (1205°C) using an extrusion ratio of 8.2:1. The as-extruded bar was pickled in a 50:50::HNO_3:H_2O solution to remove the steel jacket; care being taken to remove all traces of the steel. From a 762.0 mm. long extruded bar, 150 to 200 mm. of material was removed from either end. The resultant bar was checked with a magnet to insure that only as-consolidated P/M alloy bar was obtained without any entrapped "folds" of steel being present (see Figure 4).

Analysis of the chemical composition of the as-extruded bar for Alloy 1 and 2 is given in Table II.

The as-extruded bar was examined by both optical and thin foil transmission metallography to ascertain carbide particle distribution, grain size, etc. This data is reported later. After ascertaining that the requisite microstructural conditions were met, the material was processed further by cold swaging.

In the case of Alloy 1, various combinations of hot and cold swaging treatments and subsequent aging treatments were preliminarily carried out. The resulting microstructure was studied by thin foil transmission electron microscopy. In the next section some of these observations are discussed. It should be emphasized that the scope of the present program was limited enough so as not to allow adequate iterative experimentation to ascertain the best thermomechanical treatment sequence and aging conditions conducive to optimized mechanical properties. Nevertheless, based on the microstructural observations, the following treatment was given to the as-extruded bar of Alloy 1:

Treatment A - As-extruded 0.7-inch (18.0 mm.) diameter bar cold swaged to 0.590-inch (15.0 mm.) diameter bar and aged for 120 hours at 1200°F (650°C).

Treatment B - As-extruded 0.7-inch (18.0 mm.) diameter bar cold swaged to 0.590-inch (15.0 mm.) diameter bar, annealed for 8 minutes at 2200°F (1204°C), water quenched, cold swaged to 0.460-inch (12.0 mm.) diameter bar and aged for 120 hours at 1200°F (650°C).

TABLE II

CHEMICAL COMPOSITIONS OF THE AS-EXTRUDED P/M BAR FOR ALLOYS 1 AND 2 IN PERCENT BY WEIGHT

(Comparison with original melt chemistry and chemistry of the as-atomized powders is provided)

	Alloy 1			Alloy 2		
	Original Heat	Powder (-100/+325)	Extruded Bar	Original Heat	Powder (-100/+325)	Extruded Bar
Ni	53.7	51.8	54.5	56.79	56.64	56.65
Cr	20.08	19.7	20.2	19.96	18.97	18.85
Co	9.41	9.66	9.62	10.04	9.95	10.17
Mo	7.10	6.97	6.80	7.06	6.94	6.84
Ta	9.53	8.57	8.77	-	0.37	0.10
Cb	-	-	0.1	7.95	7.27	7.10
C	0.04	0.036	0.038	0.143	0.14	0.159
Fe	<0.2	<0.2	0.14	<0.01	0.18	0.18
O	-	0.0160	0.0146	0.0041	0.0071	0.0182
S	-	-	0.005	-	-	0.009
P	-	-	0.004	-	-	0.002
N	-	-	0.029	<0.01	-	0.013
Al	-	-	<0.1	0.14	0.02	0.02
Ti	-	-	<0.1	0.02	-	<0.02

Microstructural examination of the material during the above processing for both Alloy 1 and 2 was carried out on cross-sections of the bar material. Thin foil microscopy was carried out on similar cross-sectional "slices" of the respective bars.

Specimens for tensile and stress-rupture tests were machined from the as cold-swaged bars and subsequently heat-treated as indicated above. Specimen geometry was in accordance with ASTM specifications. The tensile specimens comprised a 1.5-inch (38.1 mm.) long specimen with 1.0-inch (25.4 mm.) gauge length and 0.16-inch (4.06 mm.) diameter in the reduced section; ends were "button heads" with a gradually tapered geometry. Stress-rupture specimens were 3-inch (76.2 mm.) long with threaded ends with a 0.250-inch (6.35 mm.) diameter in the reduced section and 1.5-inch (38.1 mm.) gauge length.

Microstructural Observations

Characterization of Powders and Consolidated Material

Figures 1a,b,c show scanning electron micrographs of the as-atomized powders of Alloy 1. The majority of particles were found to be spherical in shape and show a surface solidification structure. In some cases finer particles of approximately 40-80 micron diameter were found to be attached to or embedded in larger particles (Figure 1c). Alloy 2 powders are shown in Figures 19a and b. In Figure 19a, the low magnification (100X) scanning electron micrograph shows that several larger particles have the finer "attached" particles and Figure 19b provides an example of the nature of the solidification structure at the particle surface. Dendrites can be seen to radiate asterically from certain nucleation points on the surface of the powder particle (Figure 19b) which resembles a spherical "micro-casting". Upon sectioning the powder particles, the dendritic structure was revealed even within the body of the particles.

In order to undertake thin foil transmission electron microscopy of individual as-atomized particles, a previously-developed technique(4) was employed. Powder particles were spread upon an adhesive tape after the adhesive side of the tape had been previously gold-plated. When this sample was placed in a nickel electroplating bath, the adhesive allowed the powder particles to stay in position and the gold-film provided adequate conductivity to enable the plating process to begin. Once the nickel electroplate was sufficiently thick to "hold" the particles, the tape backing could be removed and the gold layer etched away. The "powder particles held in nickel plate" sample was further electroplated to provide a firm specimen approximately 0.004-inch (1.0 mm.) thick. Discs, 3 mm. diameter, cut from this sample were then electropolished in twin-jets of electrolyte so that a "dimple" was created on either side of the 3 mm. disc. Figure 2 shows an optical micrograph of an as-dimpled disc. When a perforation appears within the electropolished dimple it is possible to examine the surrounding edge by 100 K.V. transmission electron microscopy and study both the thinned electrolytic nickel plate and the thinned powder particles. Figures 3 and 20a and b

provide examples of the thin foil microstructure of individual powder particles of Alloys 1 and 2, respectively. The dendritic solidification structure shown in the scanning electron micrographs (Figures 1a,b,c and 19a,b) is now revealed to have a primary carbide phase associated within the dendrites. These carbides were found to be MC type carbides where, presumably, M is predominantly tantalum in Alloy 1 and predominantly columbium in Alloy 2. It is also worth noting that the carbides in the as-atomized particles are platelets. This is shown in Figure 20b where the matrix material surrounding the carbide has been etched away. In the as-atomized powders, dislocation tangles can be seen (Figure 20a) which indicate that during the solidification some thermally-induced strains have occurred.

As indicated in the previous section, after the as-atomized powder particles had been microstructurally analyzed the material was canned and extruded. In Figure 4, a photograph of the as-extruded and de-canned bars is shown. The end regions of the extruded bars were removed to eliminate any "folds" of steel and a cross-section "slice" of the consolidated P/M bar taken for microstructural examination. Figure 5a and 21a are optical micrographs of the as-extruded P/M bar for Alloys 1 and 2, respectively. Since the extrusion temperatue was 2200°F (1205°C), the as-extruded bar has essentially a recrystallized matrix. The thin foil transmission electron micrographs in Figure 5b and c (Alloy 1) and 21b and c (Alloy 2) clearly show the recrystallized structure. It is worth noting that the carbide particles and platelets in the as-atomized powders (see Figures 3 and 20a and b) are greatly refined after extrusion and there is a well-distributed morphology of MC carbide particles ranging in size from 0.25 micron to 1.0 micron. A low dislocation density can be observed in the as-extruded material (see Figure 5c).

Heat Treatment of Extruded Material

Some preliminary heat treatments were carried out on the as-extruded P/M bar for both Alloy 1 and Alloy 2 to ascertain the behavior of the Ni_3Ta (Alloy 1) and Ni_3Cb (Alloy 2) strengthening precipitates and in particular, to ascertain the change in size and morphology of the strengthening precipitates with aging time and temperature.

Figures 6a and b are thin foil micrographs of Alloy 1 extruded P/M bar which had heat treatments of 71 hours at 1450°F (790°C)(Figure 6a) and 2.75 hours at 1450°F (790°C) plus a further 64 hours at 1200°F (650°C)(Figure 6b). The body-centered tetragonal Ni_3Ta precipitate can be seen to exist in a well-distributed, homogenously-nucleated, intragranular morphology. The precipitate is in the form of platelets. In Figure 6a the Ni_3Ta platelets are approximately 4000Å in length and still maintain coherency with the matrix. In Figure 6b the two-stage heat treatment has been manifested in a bimodal morphology of the Ni_3Ta precipitate - the coarser 1450°F (790°C) platelets can be clearly seen surrounded by a much finer 1200°F (650°C) Ni_3Ta precipitate.

In analogy to the above results with Alloy 1 P/M bar, Figures 22a and b and Figures 23a,b,c show the microstructure of Alloy 2 P/M bar after heat treatment at various temperatures. Here again the coherency of the Ni_3Cb precipitate was confirmed at the various aging temperatures ranging from 1150°F to 1350°F (620°C to 730°C).

Comparing the coarser platelet-like precipitate (e.g., 4000Å size of Ni_3Ta in Figure 6a or the 3000Å size of Ni_3Cb in Figure 23a) with the fine precipitate (e.g. "1200°F" (650°C) Ni_3Ta in Figure 6b or the "1200°F" (650°C) Ni_3Cb in Figure 23c) found after treatment at lower aging temperatures, it appeared that the best strength levels from the present alloy systems would be obtained when the heat treatments caused a finer precipitate morphology to occur in the microstructure. However, to avoid a completely arbitrary choice of heat treatment conditions under which the limited testing allowed under the program would be performed, a few "quick-check" tensile tests were carried out. Material in as-extruded and variously aged conditions was tested at 1200°F (650°C) and it was revealed that the precipitation-strengthening effects of the Ni_3Ta (Alloy 1) or Ni_3Cb (Alloy 2) precipitates superimposed on a fully recrystallized (as-extruded) matrix would not be adequate to approach the 1200°F (650°C) yield strength of 200,000 psi (1373.2 MN/m^2) sought in this program.

In view of the above data, coupled with the fact that the scope of the present program excluded any systematic evaluation of the best thermo-mechanical processing sequence prior to the precipitation-strengthening heat treatment, it was decided to process the as-extruded material by cold-swaging and subsequently utilize heat-treatments which would give a fine morphology of the strengthening precipitate. The next paragraphs describe the processing procedure adopted.

Further Processing of Extruded Bars

The as-extruded P/M bars for both Alloy 1 and Alloy 2 were further processed by cold-swaging. In the case of Alloy 1, the 0.7-inch (18.0 mm) diameter extrusion was directly cold-swaged to 0.590-inch (15.0 mm) diameter. The optical microstructure of this material is shown in Figure 7a. A portion of this bar was heat-treated for 8 minutes at 2200°F (1205°C), water quenched, and further cold-swaged to 0.460-inch (11.18 mm) diameter. The optical microstructure of this heavily cold-swaged material is shown in Figure 7b. Both sets of bars were heat-treated for 120 hours at 1200°F (650°C). Figure 8a shows an optical micrograph of the smaller bar after this aging treatment (Treatment B) with a corresponding plastic replica micrograph shown in Figure 8b and thin foil micrographs in Figures 8c and 8d. A fine Ni_3Ta precipitation can be seen in the thinned samples where the extinction contours of the foils allow the correct contrast conditions to occur. Figure 10a is anoptical micrograph of the 0.590-inch (15.0 mm) bar as cold-swaged and aged for 100 hours at 1200°F (650°C) Treatment A). Comparison of Figures 8a and 10a clearly reveals the difference

in grain size and the degree of cold work. In Figure 8a (Treatment B) the grain size varies from 30-40 microns whereas in Figure 10a (Treatment A) the grain size varies from 60-75 microns. Further, even in these optical micrographs the deformation bands decorated by precipitation are clearly more copious in Figure 8a than in Figure 10a.

Tensile tests were carried out on Alloy 1 specimens in both the above conditions: Treatment A (Figure 10a) and Treatment B (Figures 8a thru d). The test data is discussed in a later section.

Alloy 2 extruded bars were cold swaged in analogy to the processing employed for Alloy 1. Instead of two different levels of cold-work and two different grain sizes as in the case of Alloy 1, only one processing treatment was employed. The as-extruded Alloy 2 P/M bar was directly cold-swaged to 0.600-inch (15.2 mm.) diameter (see micrograph in Figure 24a), annealed for 8 minutes at 2200°F (1205°C), quenched and further cold swaged to 0.495-inch (12.8 mm.) diameter (see micrograph in Figure 24b). Figure 24c shows the thin foil microstructure of a cross-section of the as-cold swaged 0.495-inch (12.8 mm.) diameter bar. The size and distribution of the CbC carbide particles is not greatly altered from that found in the as-extruded bar (compare Figure 24c and Figure 21c). The as-cold-swaged bar was then heat treated for 120 hours at 1200°F (650°C). Figure 25a shows an optical micrograph of the as heat treated alloy 2 bar in which the deformation bands can be seen to be decorated by precipitation. In Figure 25b, the thin foil microstructure confirms the existence of fine Ni_3Cb precipitate on the deformed structure (compare with Ni_3Ta in Figures 8c and d). Alloy 2 specimens were tested in this condition as is discussed later.

In addition to the precipitation-strengthening heat treatments given to the cold-swaged specimens of Alloy 1 and 2, some specimens in each case were further exposed for 100 hours at 1400°F (760°C) as a test of stability. As reported later, tensile properties have been evaluated on these "1400°F (760°C) exposure" samples. Here it is necessary to note some of the microstructural observations on the "as-strengthened" material after further exposure at 1400°F (760°C) for 100 hours.

Figures 9a,b,c and d show the microstructure of Alloy 1 P/M bar as extruded, cold-swaged (with intermediate anneal) to 0.460-inch (11.65 mm.) diameter, aged for 120 hours at 1200°F (650°C) (Treatment B) and then exposed for 100 hours at 1400°F (760°C). Figure 9a shows an optical micrograph which when compared to Figure 8a shows that further precipitation at grain boundaries has occurred. The replica micrograph in Figure 9b and thin foil micrographs in Figures 9c and d clarify the effects of the 100 hours at 1400°F (760°C) exposure. In limited regions (e.g., at "B" in Figures 9c and d) a recrystallization effect is seen to occur together with a transformation of Ni_3Ta tetragonal strengthening precipitate to orthorhombic Ni_3Ta acicular phase (see Appendix A). This transformation is not found in the

case of material with an undeformed matrix where the Ni_3Ta body-centered-tetragonal precipitate retains its coherency even after 100 hours at 1500°F (816°C). Therefore, it appears that the "recrystallization" cells in the present samples after 100 hours exposure at 1400°F (760°C) are due to the work introduced prior to the 120 hours at 1200°F (650°C) strengthening heat treatment. As will be discussed later, this recrystallization does not have any deleterious effect on ductility. Also, by a more complete study of the thermomechanical processing prior to aging it should be possible to partially eliminate the high degree of pre-precipitation cold work used in the present processing sequence without sacrificing the strength levels obtained (see later section) and, thereby, avoid this "recrystallization" problem at 1400°F (760°C) for Alloy 1.

The Ni_3Cb precipitate in Alloy 2 is inherently less stable at 1400°F (760°C) than the Ni_3Ta precipitate in Alloy 1. After 1400°F (760°C) exposure for 100 hours, the material cold worked and aged for 120 hours at 1200°F (650°C) recrystallized as is shown in Figures 26a (optical micrograph) and 26b (thin foil electron micrograph). As suggested by these microstructural observations, the strength levels after exposure for 100 hours at 1400°F (760°C) are also substantially reduced (see later text). It should be noted that recrystallization occurs in Alloy 2 at 1400°F (760°C), even when the previous 1200°F (650°C) aging treatment (which forms the strengthening Ni_3Cb precipitate) is superimposed on an undeformed matrix. In either case the Ni_3Cb body-centered-tetragonal precipitate does transform to acicular laths of Ni_3Cb precipitate. Thus, in terms of microstructural stability at 1400°F (760°C) it appears that of the two compositions evaluated here, Alloy 1 (Ni_3Ta strengthened) is certainly superior to Alloy 2 (Ni_3Cb strengthened) and this is confirmed by the mechanical properties data reported infra.

Alloy Testing and Post-Testing Metallography

As indicated above, Alloy 1 was tested in two conditions, viz., Treatment A where a 0.590-inch (15.0 mm.) diameter cold-swaged bar was aged to 120 hours at 1200°F (650°C), and Treatment B where a bar cold-swaged to 0.460-inch (11.7 mm.) diameter was aged for 120 hours at 1200°F (650°C). Also as noted earlier, the grain size was 60-75 microns for Treatment A and 30-40 microns for Treatment B.

Duplicate tensile tests were conducted at room temperature, 1200°F (650°C) and 1400°F (760°C) for the material after Treatment B and for purposes of comparison single tensile tests were conducted at the same temperatures for material after Treatment A. These tensile data are tabulated in Table III, and are shown graphically in Figures 11, 12, 13, and 14. It is worth noting that the 1200°F (650°C) yield strength for Alloy 1 after Treatment B (see Figure 12) is ~188,000 psi (1290 MN/m^2), with better than 10 percent tensile elongation and better than 15 percent reduction in cross-sectional area.

TABLE III

TENSILE DATA FOR ALLOY 1

Test No.	Date	Test Temp. °F	Test Temp. °C	Yield Stress psi	Yield Stress MN/m^2	Ultimate Stress psi	Ultimate Stress MN/m^2	Elongation %	R. of Area %
				AFTER TREATMENT A					
41211	8/21/69	RT		216,100	1484.0	232,700	1598.0	10.3	24.6
41213	8/21/69	1200	650	175,600	1206.0	195,500	1342.0	9.4	14.4
41215	8/21/69	1400	760	151,100	1037.0	156,200	1072.0	6.7	6.5
				AFTER TREATMENT B					
41212	8/21/69	RT		241,800	1660.0	253,200	1738.0	8.4	25.4
41284	9/30/69	RT		249,751	1715.0	261,194	1793.0	3.3	7.5
41214	8/21/69	1200	650	188,050	1291.0	207,450	1424.0	15.5	21.4
41188	8/4/69	1200	650	188,750	1296.0	212,500	1459.0	11.2	18.5
41216	8/21/69	1400	760	147,600	1013.0	154,150	1058.0	4.7	2.5
41286	9/30/69	1400	760	134,328	922.0	159,204	1093.0	5.1	3.5
				TREATMENT A + 100 HRS. AT 1400°F					
41234	8/29/69	RT		204,522	1404.0	224,623	1542.0	14.6	22.6
41236	8/29/69	1200	650	168,159	1155.0	194,527	1336.0	15.8	19.9

TABLE III (Continued)

Test No.	Date	Test Temp. °F	Test Temp. °C	Yield Stress psi	Yield Stress MN/m^2	Ultimate Stress psi	Ultimate Stress MN/m^2	Elongation %	R. of Area %
				TREATMENT B + 100 HRS. AT 1400°F					
41235	8/29/69	RT		222,600	1528.0	237,688	1632.0	13.6	29.1
41237	9/30/69	RT		209,493	1438.0	239,303	1643.0	7.0	17.9
41237	8/29/69	1200	650	174,627	1199.0	197,015	1353.0	15.4	15.4
41288	10/1/69	1200	650			Specimen was flawed			

Table III also includes data from room temperature and 1200°F (650°C) tensile tests on Alloy 1 material both in "Treatment A" and "Treatment B" conditions plus an additional 100 hours at 1400°F (760°C) exposure. The data shows that in the "best strength" condition (i.e., Condition "B") the material retains 92 percent of 1200°F (650°C) yield strength even after the 100 hours at 1400°F (760°C) exposure without loss of ductility. This reinforces the observation made in the previous section that although there are "recrystallization" cells observed adjacent to grain boundaries (see Figures 9b,c,d) after exposure at 1400°F (760°C) for 100 hours, there is no deleterious effect on ductility. Some Alloy 1 specimens after Treatment B were tested in stress rupture at 1200°F (650°C) (see Figures 18a and b). The following data (Table IV) was obtained:

TABLE IV

STRESS RUPTURE TESTS FOR
Alloy 1 After Treatment B

Test No.	Date	Test Temp. °F	Test Temp. °C	Stress Level p.s.i.	Stress Level MN/m^2	Life in Hours
10266	10/15/69	1200	650	110,000	755.0	26.2
10255	10/10/69	1200	650	110,000	755.0	37.5
10189	9/5/69	1200	650	150,000	1030.0	3.2
10224	9/22/69	1200	650	150,000	1030.0	4.4

As stated earlier, for Alloy 2, duplicate tensile tests at room temperature, 1200°F (650°C) and 1400°F (760°C) were carried out on material which was extruded, cold-swaged (with intermediate anneal) to .495-inch (12.6 mm.) diameter, and aged for 120 hours at 1200°F (650°C) and also duplicate tests at room temperature and 1200°F (650°C) on material which was further exposed 100 hours at 1400°F (760°C). This data is tabulated in Table V and graphically represented in Figures 30 and 31.

The tensile properties of Alloy 2 confirm the microstructural observations reported in the previous section. As in the case of Alloy 1, the 1200°F (650°C) yield strength of Alloy 2 is at a high level (~189,000 psi (1300 MN/m^2)) with greater than 10 percent tensile elongation and greater than 15 percent reduction in cross-sectional area. However, in contrast to Alloy 1, the 1400°F (760°C) tensile yield strength of Alloy 2 falls off abruptly. In Alloy 1, a 1200°F (650°C) tensile yield strength of ~189,000 psi (1300 MN/m^2) decreases to a 1400°F (760°C) tensile yield strength of ~145,000 psi (1010 MN/m^2), whereas in Alloy 2, the respective strength levels are

TABLE V

TENSILE DATA OF ALLOY 2

Test No.	Date	Test Temp. °F	Test Temp. °C	Yield Stress psi	Yield Stress MN/m^2	Ultimate Stress psi	Ultimate Stress MN/m^2	Elongation %	R. of Area %
				AFTER STRENGTHENING HEAT-TREATMENT					
43263	11/12/69	RT		243,580	1672.0	259,700	1783.0	5.0	15.4
43264	11/12/69	RT		241,800	1660.0	257,100	1765.0	3.4	13.4
43265	11/12/69	1200	650	161,050	1106.0	191,540	1315.0	25.2	18.0
43488	12/2/69	1200	650	182,900	1256.0	200,000	1373.0	12.0	25.5
43615	12/26/69	1200	650	189,100	1298.0	209,000	1435.0	14.5	18.9
43267	11/12/69	1400	760	85,970	590.0	99,500	683.0	22.3	28.1
43268	11/12/69	1400	760	83,580	574.0	101,000	693.0	23.9	27.2
				AFTER ADDITIONAL EXPOSURE OF 100 HRS. AT 1400°F					
43320	11/24/69	RT		158,800	1090.0	200,000	1373.0	9.3	14.4
43321	11/24/69	RT		166,300	1142.0	203,400	1397.0	10.3	16.9
43322	11/24/69	1200	650	111,900	768.0	133,300	915.0	16.1	15.4
43323	11/24/69	1200	650	105,100	722.0	128,600	883.0	13.1	15.4

~189,000 psi (1300 MN/m^2) and ~85,000 psi (590 MN/m^2). This behavior is confirmed by the microstructural observation on the specimens after testing.

Figures 15a,b, 16a,b, and 17a,b are thin foil micrographs cross-sectional "slices" taken from the gauge-length of Alloy 1 tensile specimens tested at room temperature, 1200°F (650°C) and 1400°F (760°C), respectively. Figures 16c and 17c are corresponding optical micrographs after 1200°F (650°C) and 1400°F (760°C) tensile tests. In each of the three test conditions (room temperature, 1200°F or 650°C and 1400°F or 760°C) the strengthening Ni_3Ta precipitate has not altered in morphology during the test nor has any transformation occurred in the crystallography of the precipitate. (The Ni_3Ta body-centered-tetragonal precipitate does exhibit some transformation to Ni_3Ta orthorhombic phase, but only when exposed at 1400°F (760°C) for long times - see earlier text and Figures 9b,c,d.) By contrast, in the case of the Ni_3Cb precipitate in Alloy 2, transformation to orthorhombic Ni_3Cb does occur during the 1400°F (760°C) tensile test. Figures 27a,b,c, 28a,b,c, and 29a,b,c are micrographs of cross-sectional slices of Alloy 2 tensile specimens tested at room temperature, 1200°F (650°C) and 1400°F (760°C), respectively.

In Figure 29c, the thin foil micrograph clearly shows that recrystallization has occurred during the 1400°F (760°C) tensile test and that laths of orthorhombic Ni_3Cb phase have formed. This clearly is the cause of the change in the yield strength of Alloy 2 from ~189,000 psi (1300 MN/m^2) at 1200°F (650°C) to ~85,000 psi (590 MN/m^2) at 1400°F (760°C). The same instability is manifested in tests on Alloy 2 material exposed for 100 hours at 1400°F (760°C) (Figure 26) where the 1200°F (650°C) yield strength of 189,000 psi (1300 MN/m^2) has decreased to 111,900 psi (768 MN/m^2) whereas in Alloy 1 the 1200°F (650°C) yield strength after the 100 hours at 1400°F (760°C) exposure (~175,000 psi or 1200 MN/m^2) was 92 percent the strength level before exposure (~189,000 psi or 1300 MN/m^2). Stress-rupture tests on Alloy 2 were carried out and the following data (Table VI) obtained.

TABLE VI

Stress-Rupture Data for Alloy 2

Test No.	Date	Test Temp. °F	Test Temp. °C	Stress Level p.s.i.	Stress Level MN/m^2	Life In Hours
10316	11/12/69	1200	650	110,000	755.0	6.7
10322	11/14/69	1200	650	110,000	755.0	9.2

DISCUSSION

The foregoing results demonstrate that a nickel-base composition, strengthened by the precipitation of a body-centered-tetragonal phase on a cold worked consolidated powder-metallurgy alloy matrix, is capable of exhibiting high levels of 1200°F (650°C) tensile yield strength required in the instant program. Of the two alloy systems investigated here, the Ni_3Ta strengthened Alloy 1 shows high 1400°F (760°C) tensile yield strengths and 92 percent retention of the 1200°F (650°C) strength levels after 100 hours exposure at 1400°F (760°C).

The Ni_3Cb strengthened Alloy 2 demonstrates a lesser degree of maintenance of strength at 1400°F (760°C) and also after exposure 100 hours at 1400°F (760°C).

In the latter case the instability of the Ni_3Cb phase in the predominant cause of the lower tensile strengths of Alloy 2 after exposure at 1400°F (760°C). In the case of Alloy 1, the body-centered-tetragonal Ni_3Ta phase is not, per se, unstable when exposed at 1400°F. However, the existence of a highly cold-worked matrix prior to precipitation does cause localized recrystallization to occur when Alloy 1 is exposed at 1400°F (760°C). This recrystallization is accompanied by limited transformation of the Ni_3Ta (b·c·tet.) to Ni_3Ta (orthorhombic) phase. By contrast, in Appendix A data is presented on the stability of Ni_3Ta in an undeformed matrix of similar composition to Alloy 1. No transformation of the body-centered-tetragonal Ni_3Ta phase to orthorhombic Ni_3Ta phase occurs in the case of the undeformed matrix even when exposed for 100 hours at 1500°F (815°C). In Appendix B, X-ray diffraction data is presented to show that the formation of orthorhombic Ni_3Ta does occur in Alloy 1 when the cold worked and precipitation strengthened (aged at 1200°F or 650°C) matrix is exposed for 100 hours at 1400°F (760°C).

This above mentioned data serves to emphasize that further improvements in the stability of Alloy 1 are possible if the presently obtained strength levels can be maintained while lessening the degree of pre-precipitation cold work. Therefore, as a subsequent and continuing investigation of the present preliminary study, it has been recommended that a program of optimizing the pre-precipitation strengthening deformation of Alloy 1 be undertaken. The goal of the envisaged investigation would be to: (a) maintain and, if possible enhance the present 1200°F (650°C) tensile yield and ultimate strength levels, while improving upon the 1400°F (760°C) stability of Alloy 1, (b) to improve the present stress rupture properties of Alloy 1 and, (c) to modify and optimize the present composition of Alloy 1 and define the compositional ranges for the resultant P/M alloy for 1000-1400°F (540-760°C) applications.

CONCLUSIONS

1. A nickel-base composition, utilizing the powder-metallurgy method and strengthened by the precipitation of a body-centered-tetragonal intermetallic phase has been defined which provides a 1200°F (650°C) strength level of 189,000 psi (1296 MN/m^2) with better than 10 percent tensile elongation.

2. Of two alloys investigated in the present investigation, Alloy 1 (which in weight percent is 54.5 Ni - 20.2 Cr - 9.62 Co - 6.80 Mo - 8.77 Ta - 0.1 Cb - 0.038 C - 0.14 Fe - 0.0146 O - 0.005 S - 0.004 P - 0.029 N - <0.1 Al - <0.1 Ti) which is strengthened by the precipitation of Ni_3Ta phase is more stable than Alloy 2 (which in weight percent is 56.65 Ni - 18.85 Cr - 10.17 Co - 6.84 Mo - 0.10 Ta - 7.10 Cb - 0.159 C - 0.18 Fe - 0.0182 O - 0.009 S - 0.002 P - 0.013 N - 0.02 Al - <0.02 Ti) which is strengthened by the precipitation of Ni_3Cb phase.

3. Microstructural analysis of the above alloy systems has indicated the causes of 1400°F instability in these precipitation strengthened systems, and it has been shown that by control of the deformation prior to precipitation-strengthening, the 1400°F (760°C) stability of Alloy 1 can be further increased.

4. Alloy 2 is not recommended for further study, but in the case of Alloy 1, a program to optimize the post-consolidation thermomechanical treatment is proposed. It is expected that with further process optimization, the present strength levels of Alloy 1 can be maintained while improving 1400°F (760°C) stability and stress-rupture behavior at 1200°F (650°C).

RECOMMENDATIONS

The results of the study demonstrate that the Ni_3Ta strengthened Alloy 1 is a viable P/M superalloy system. The body-centered-tetragonal Ni_3Ta phase per se is stable up to 1500°F (815°C)(see Appendix A). However, when the matrix is extensively cold worked prior to precipitation of Ni_3Ta, the alloy shows the commencement of recrystallization at 1400°F (760°C) and the existence of cold work in the matrix enhances the formation of orthorhombic Ni_3Ta. Therefore, as a subsequent and continuing investigation of the present preliminary study, it is recommended that a program of optimizing the pre-precipitation strengthening deformation of Alloy 1 be undertaken. The goal of the envisaged investigation would be to:

a. Maintain and, if possible enhance the present 1200°F (650°C) tensile yield and ultimate strength levels, while improving upon the 1400°F (760°C) stability of Alloy 1.

b. Improve the present stress rupture properties of Alloy 1.

c. Modify and optimize the present composition of Alloy 1 and define the compositional ranges for the resultant P/M alloy for 1000-1400°F (540-760°C) applications.

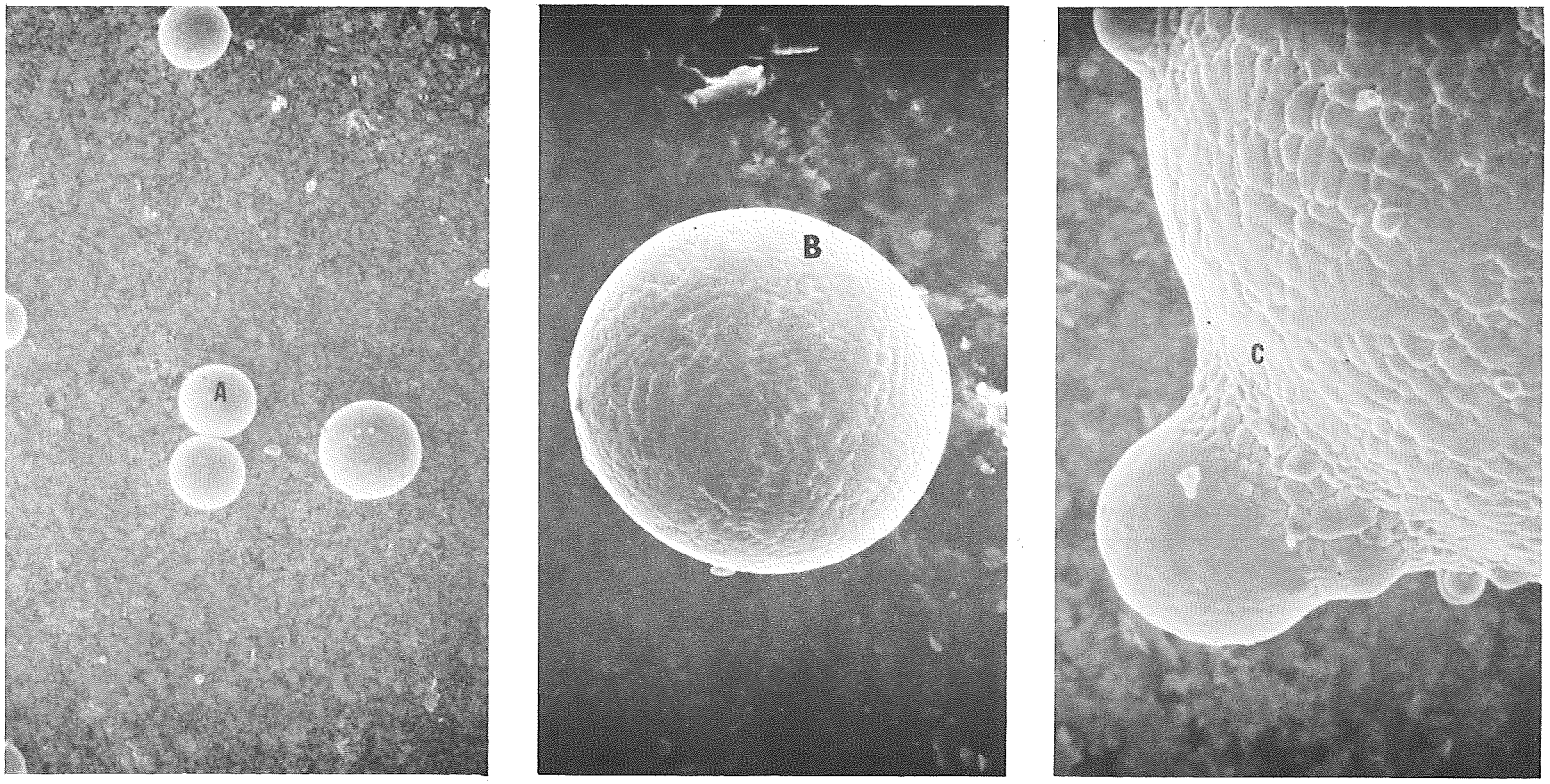

Figure 1. Alloy 1 powder. Scanning electron micrographs show atomized powders. 100/325 mesh fraction particles are shown. (A) 100x, (B) 1000x, (C) 1000x.

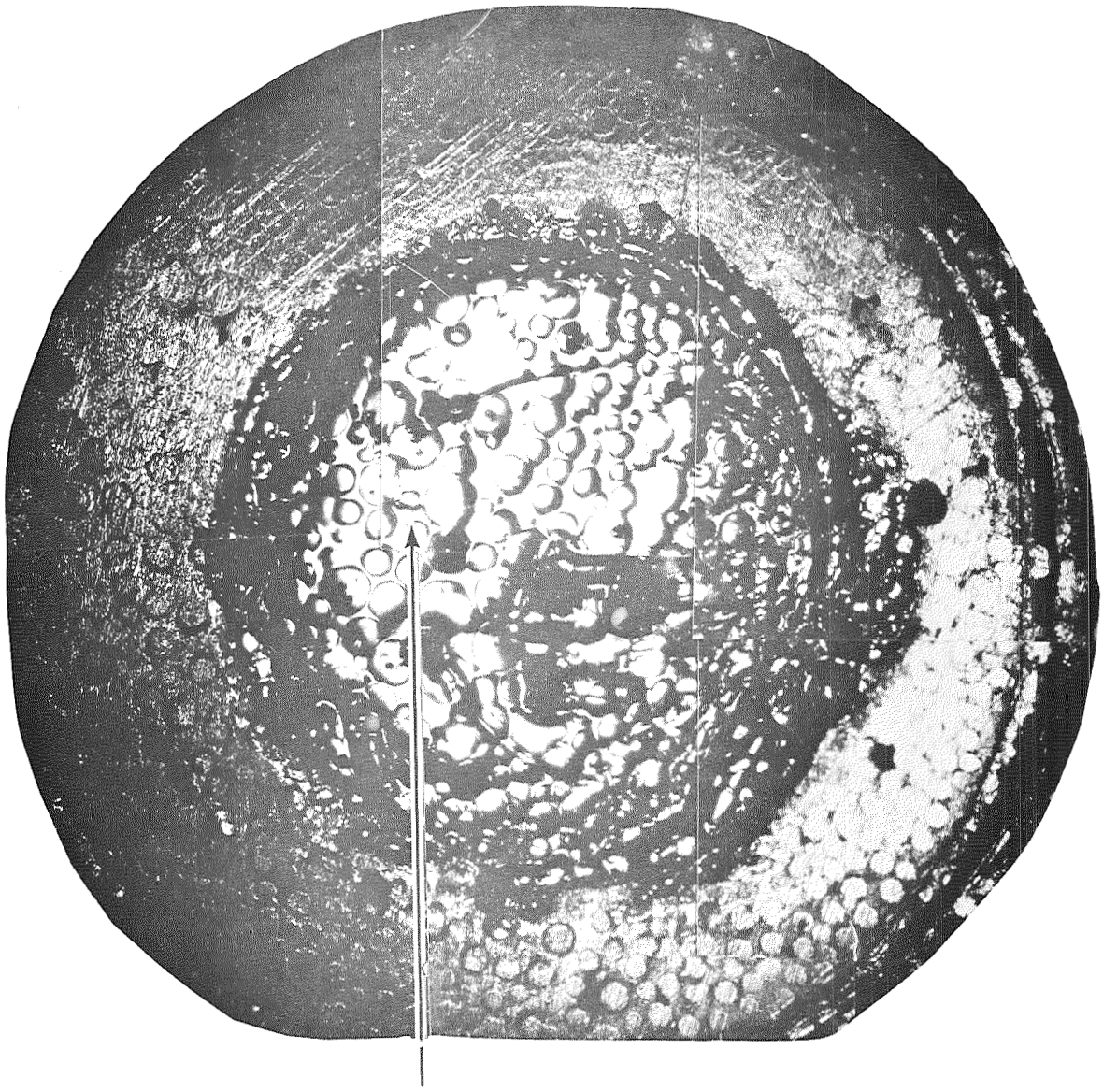

Figure 2. Optical micrograph of a 3mm diameter disc from a 0.003 inch thick sheet of electrolytic nickel plate in which particles of Alloy 1 powders have been "held". The disc has been dimpled for electropolishing with twin jets.

Figure 3. Thin foil micrograph of an individual particle of Alloy 1 powder. Prepared by using a sample as shown in Figure 2. 25,000x.

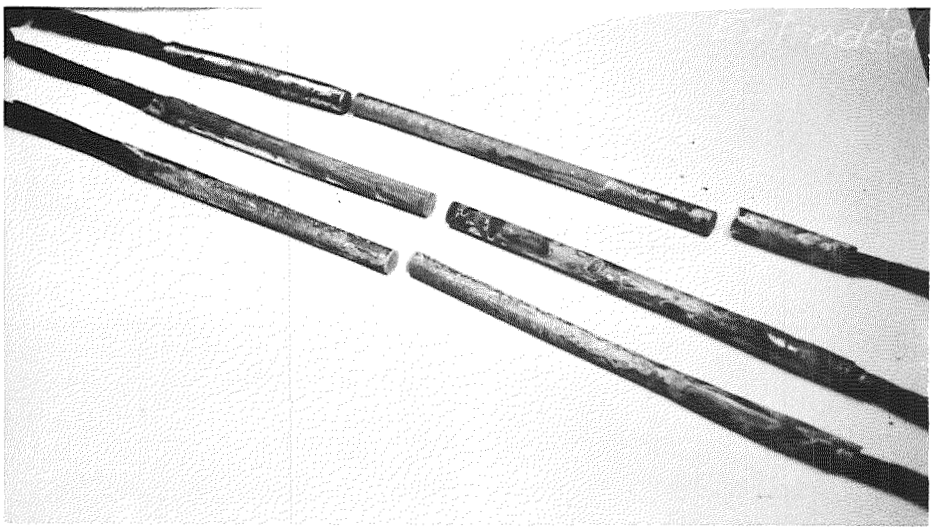

Figure 4. Photograph showing Alloy 1 bars after extrusion and decanning.

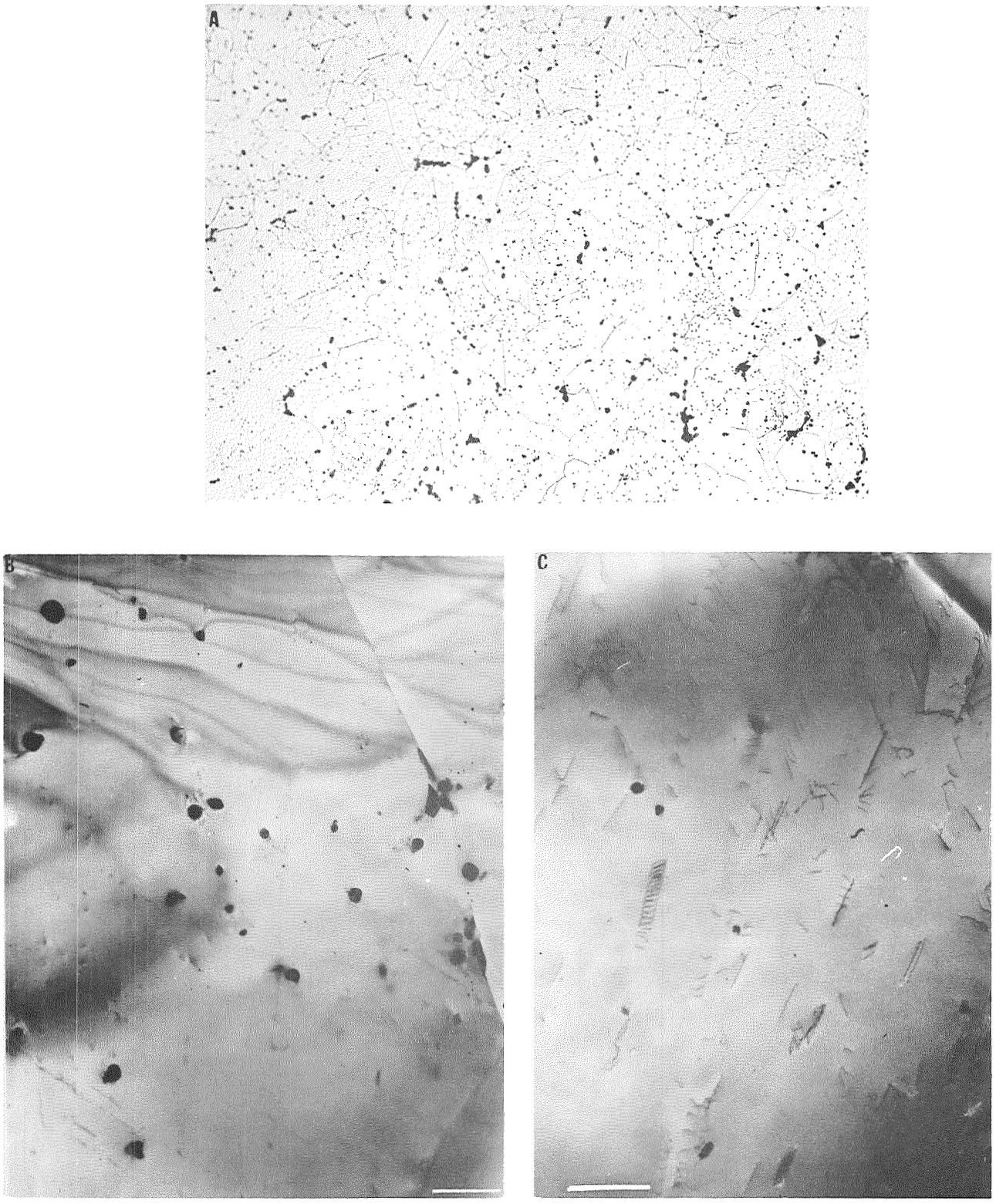

Figure 5. (A) Optical micrograph showing the microstructure of as-extruded Alloy 1 bar. 500x. (B) and (C) Thin foil micrographs of a cross section of as-extruded bar. Note the fine distribution of primary carbide particles and the low dislocation density. The line marks on the micrographs represen one micron.

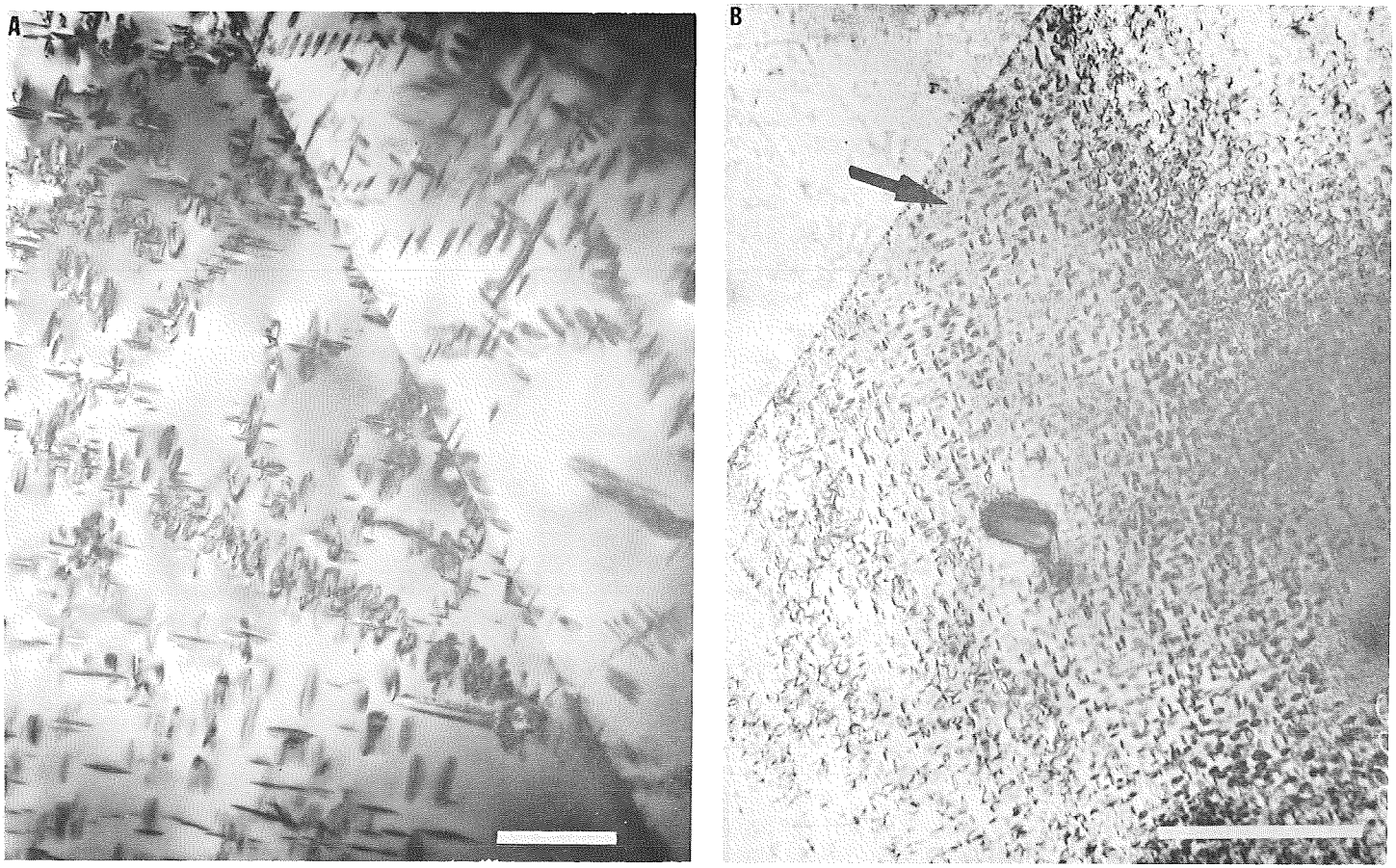

Figure 6. A. Thin foil micrograph of Alloy 1 as-extruded and aged for 71 hours at 1450° F. B. Thin foil micrograph of Alloy 1 bar as-extruded and aged 2.75 hours at 1450° F and further aged for 64 hours at 1200° F. Line marks on each photograph represent one micron. In micrograph B the arrow shows the fine 1200° F precipitate surrounding the coarser 1450° F.

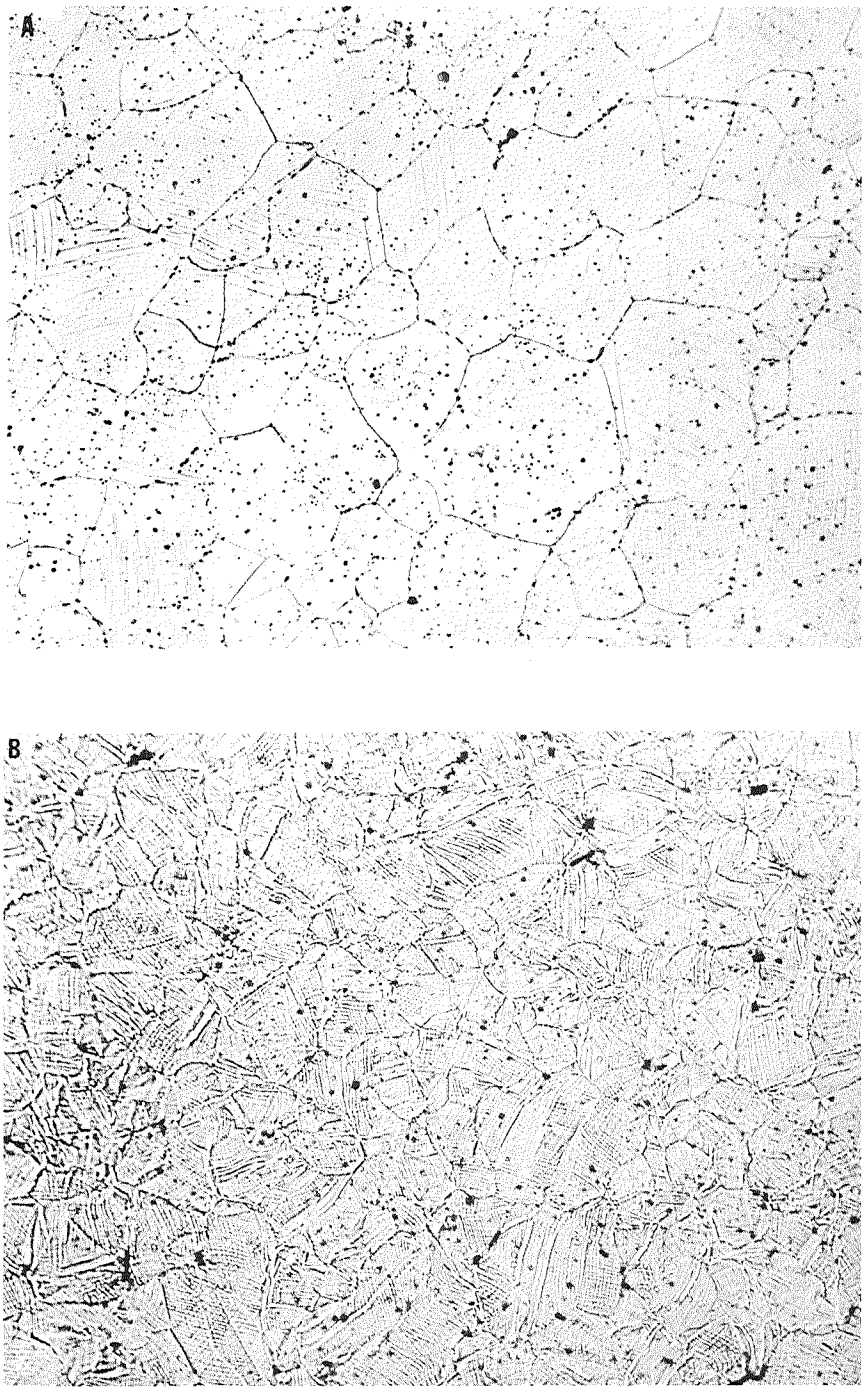

Figure 7. Optical micrographs of as-extruded and cold swaged Alloy 1 bar. (A) The cross section of rod as-extruded and directly cold swaged to .590 inch diameter. (B) Cross section of rod annealed for 8 minutes at 2200° F in the condition shown in (A) above and then further cold swaged to .460 inch diameter. Both at 500x.

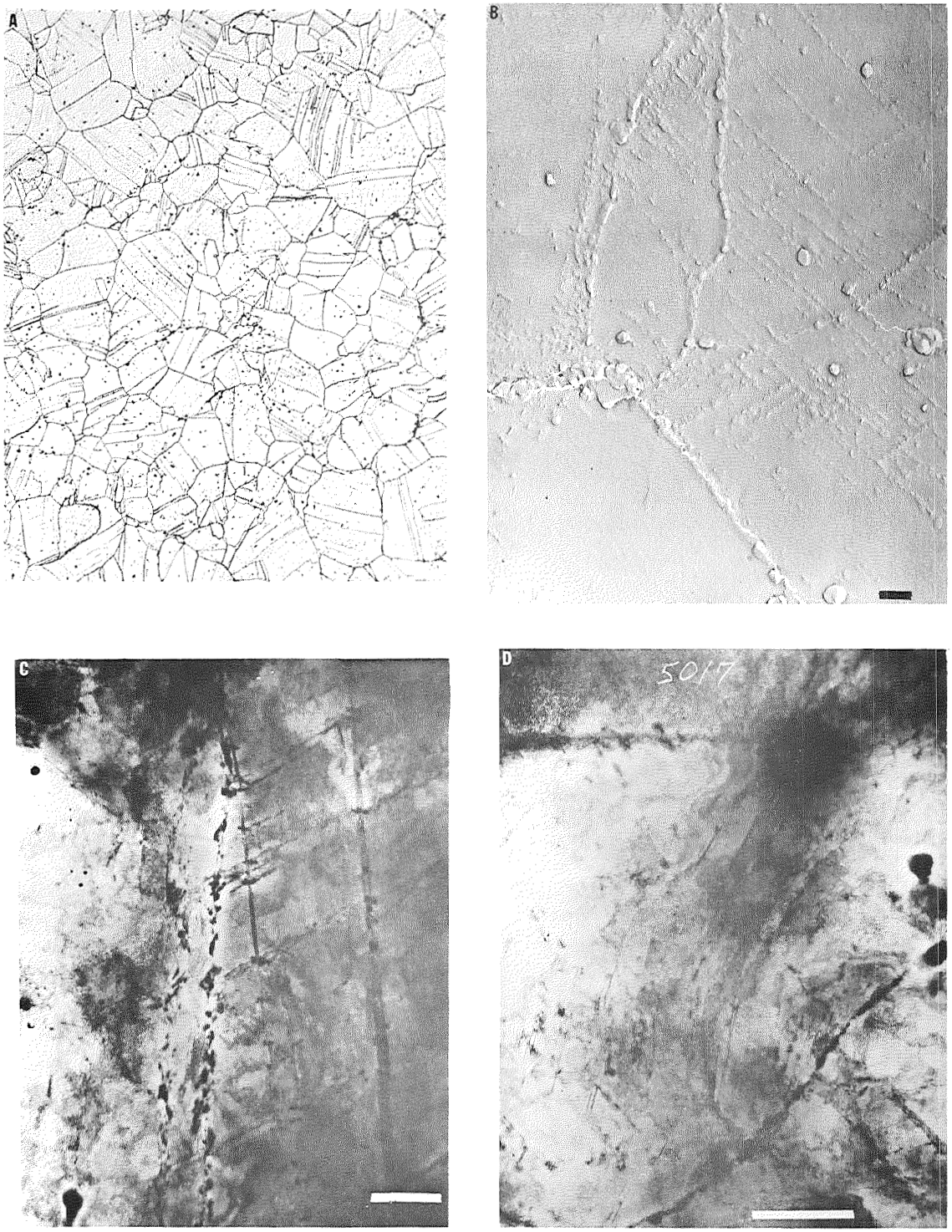

Figure 8. (A) Optical micrograph of Alloy 1 rod cold swaged to .460 inch diameter (cf Figure 7 (B) above) and aged for 120 hours at 1200° F. 500x. (B) Plastic replica of Alloy 1 bar in same condition as in (A) above. (C) and (D) Thin foil micrographs of Alloy 1 bar as cold swaged to .460 inch diameter and then aged for 74.5 hours at 1200° F. The line marks on micrographs 8 (B), 8 (C) and 8 (D) represent one micron.

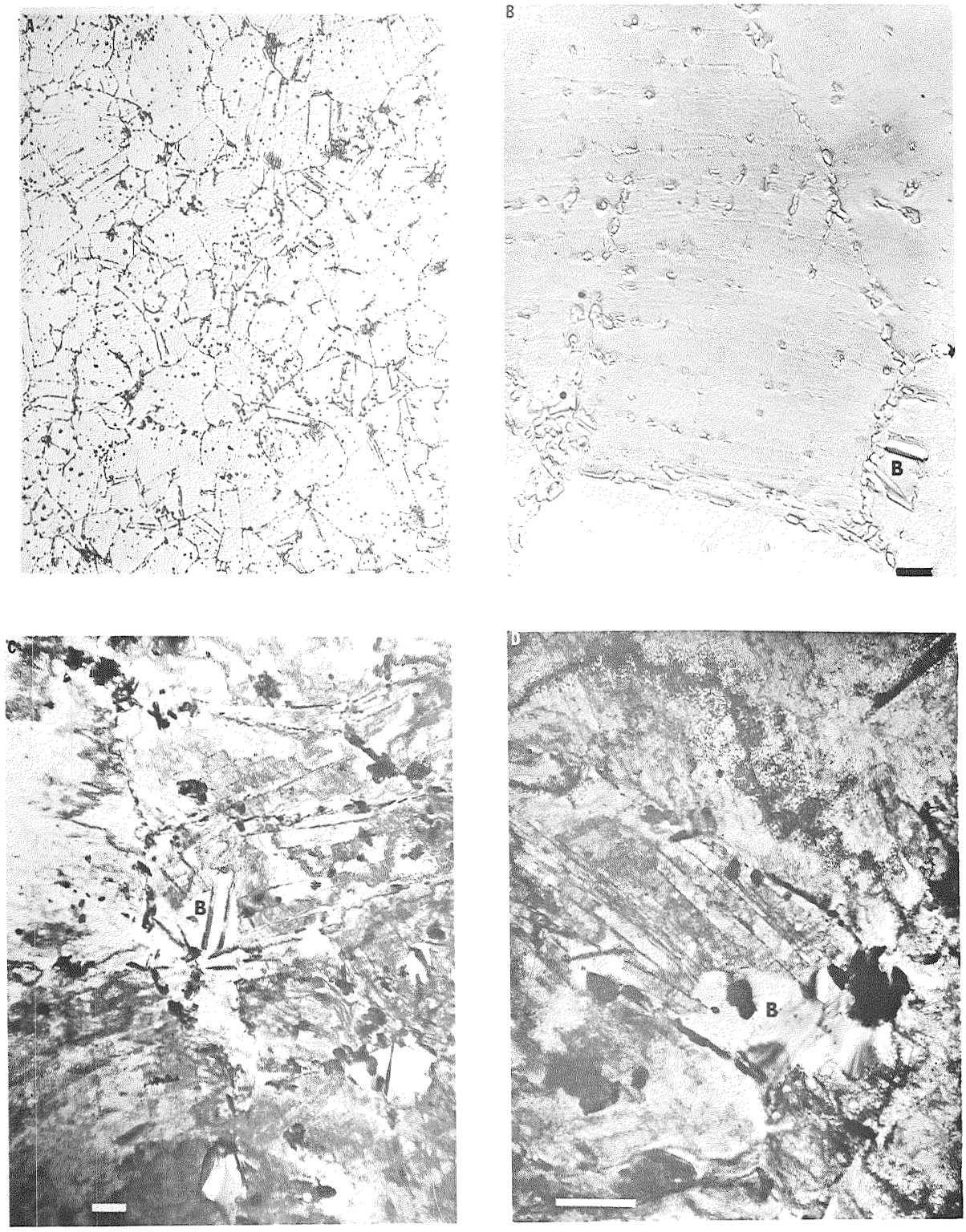

Figure 9. (A) Optical micrograph of Alloy 1 bar cold swaged to .460 inch diameter aged 120 hours at 1200° F and further exposed for 100 hours at 1400° F. 500x. (B) Plastic replica of Alloy 1 material as in (A) above. The regions marked "B" in Figures 9 (B), 9 (C) and 9 (D) seem to represent the beginning of secondary recrystallization. (See text.) Line marks on Figures 9 (B), 9 (C) and 9 (D) represent one micron.

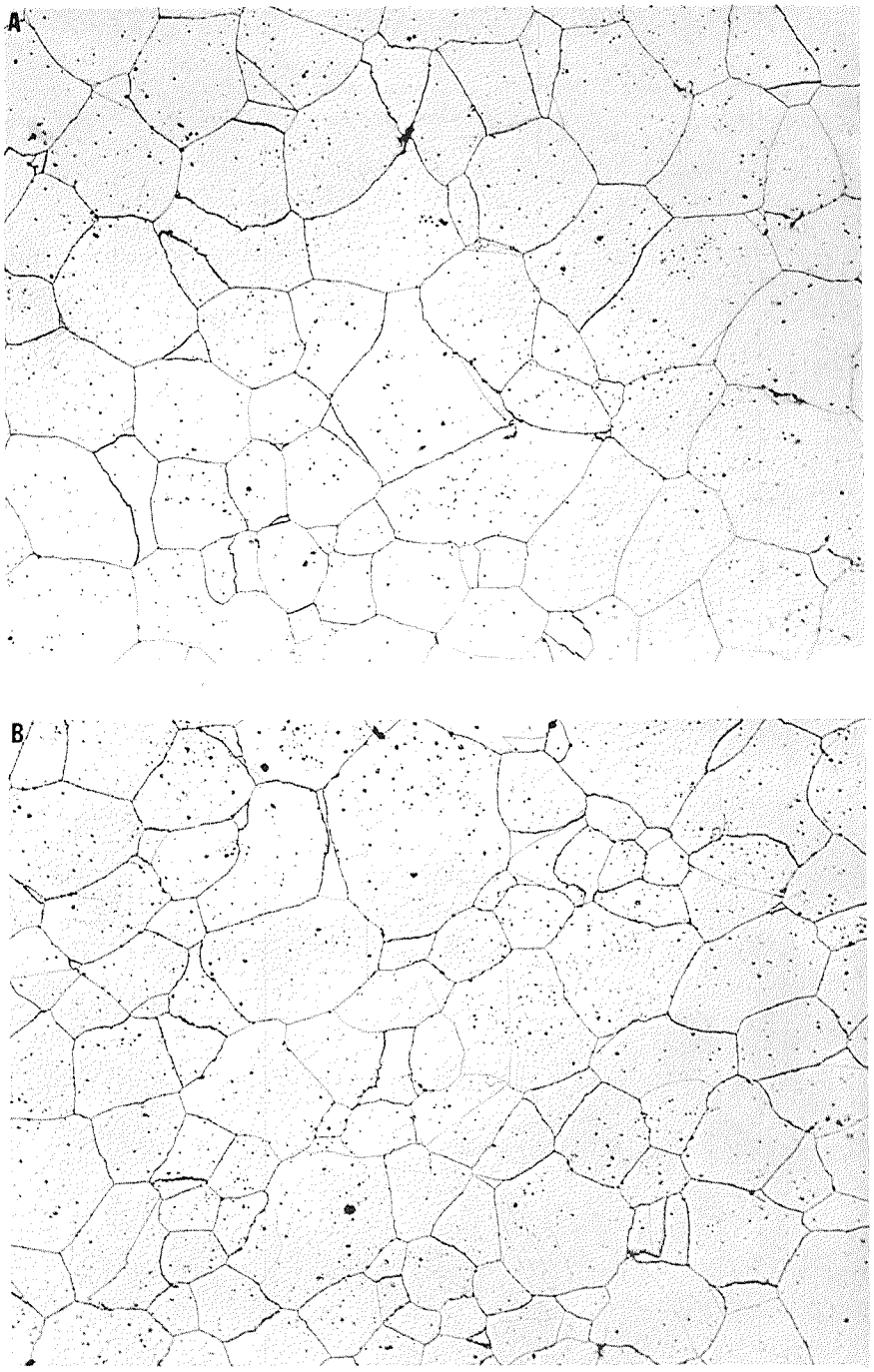

'igure 10. Optical micrograph of Alloy 1 bar as-extruded and directly cold swaged to .590 inch diameter and then (A) aged for 120 hours at 1200° F and (B) aged for 120 hours for 1200° F and further aged for 100 hours at 1400° F. 500x.

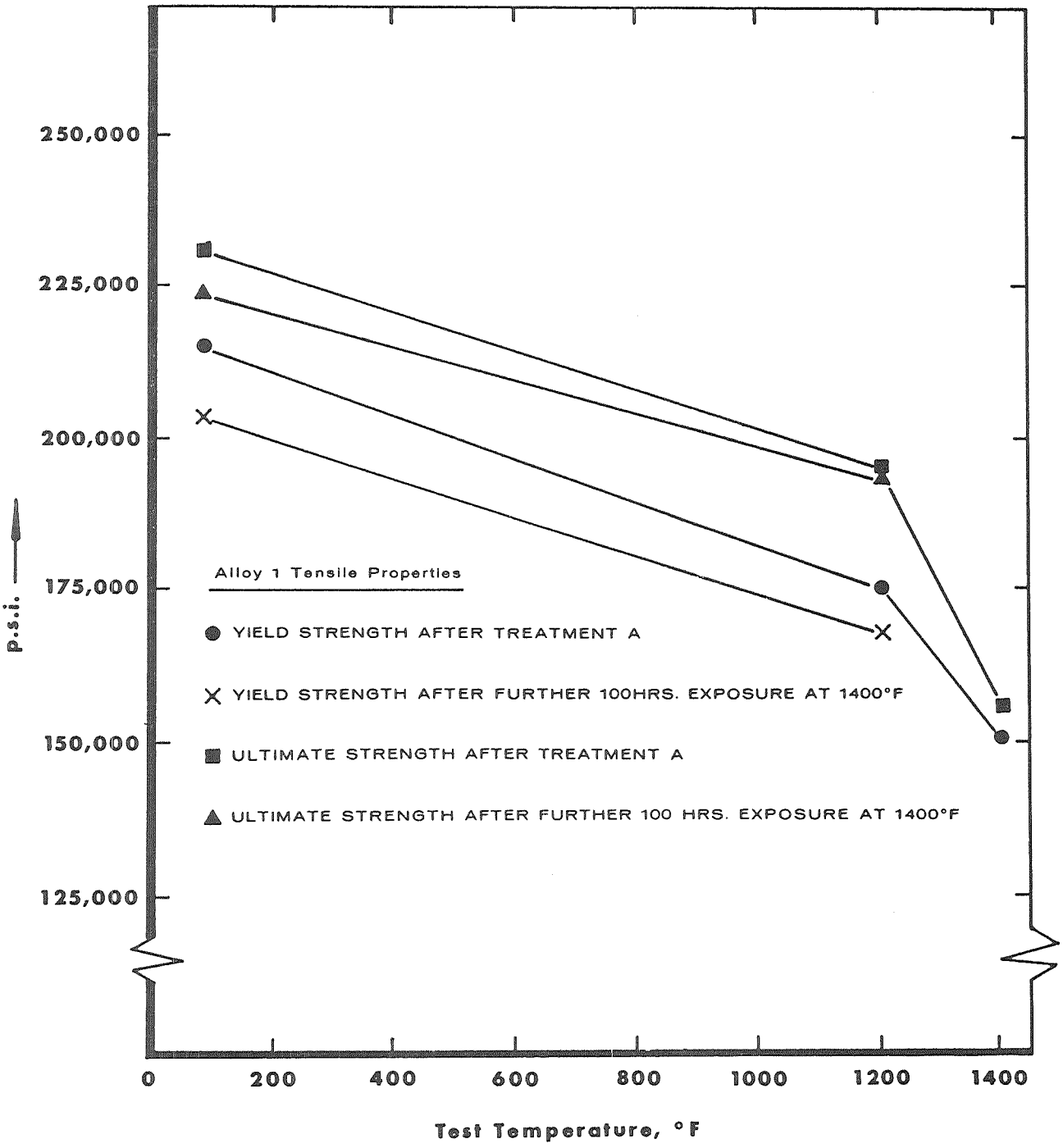
250,000
225,000
200,000
175,000
150,000
125,000
p.s.i.
Alloy 1 Tensile Properties
YIELD STRENGTH AFTER TREATMENT A
YIELD STRENGTH AFTER FURTHER 100HRS. EXPOSURE AT 1400°F
ULTIMATE STRENGTH AFTER TREATMENT A
ULTIMATE STRENGTH AFTER FURTHER 100 HRS. EXPOSURE AT 1400°F
0
200
400
600
800
1000
1200
1400
Test Temperature, °F

Fig. 11.

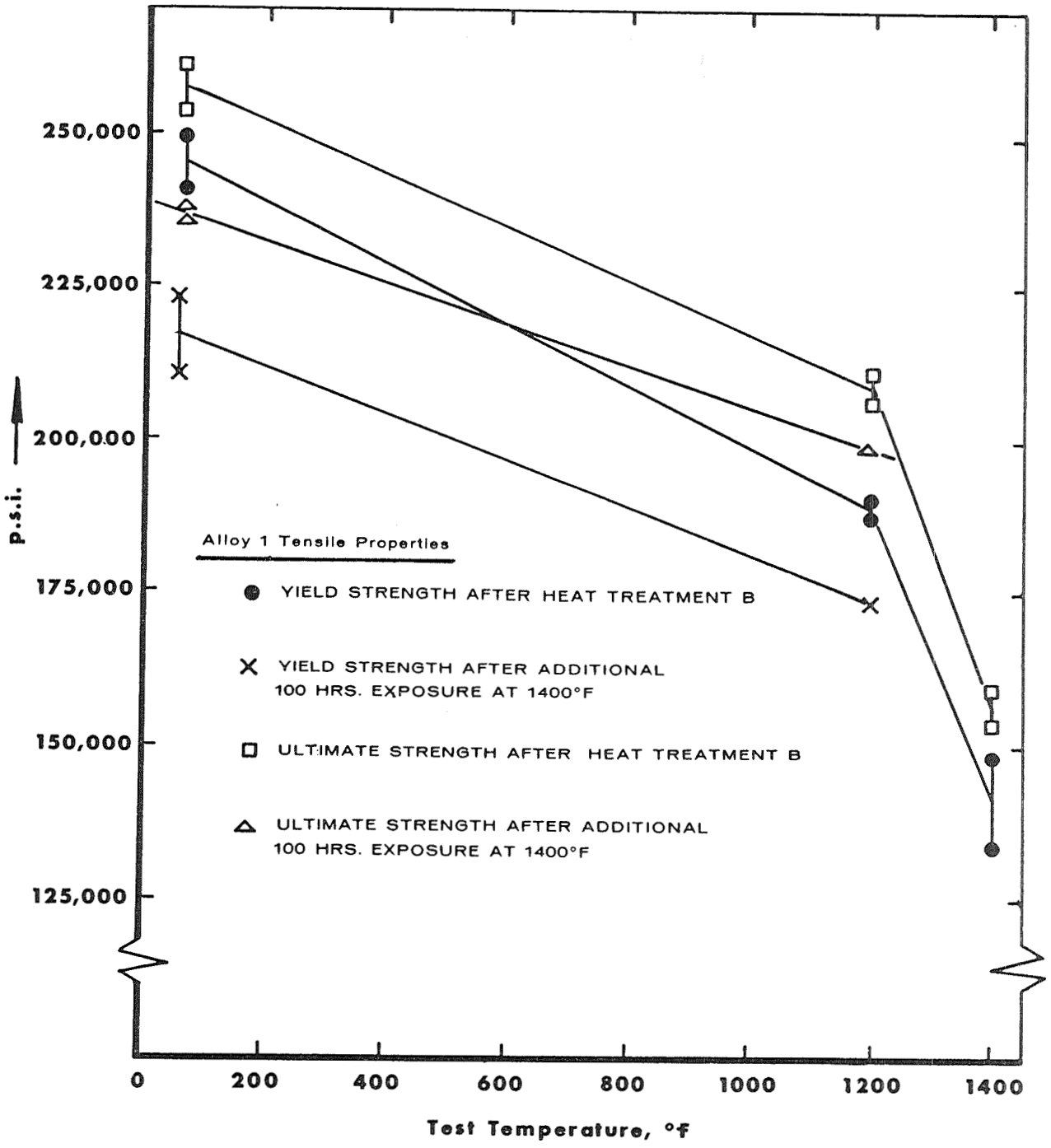
250,000
225,000
200,000
175,000
150,000
125,000
p.s.i.
Alloy 1 Tensile Properties
YIELD STRENGTH AFTER HEAT TREATMENT B
YIELD STRENGTH AFTER ADDITIONAL 100 HRS. EXPOSURE AT 1400°F
ULTIMATE STRENGTH AFTER HEAT TREATMENT B
ULTIMATE STRENGTH AFTER ADDITIONAL 100 HRS. EXPOSURE AT 1400°F
0
200
400
600
800
1000
1200
1400
Test Temperature, °F

Fig. 12.

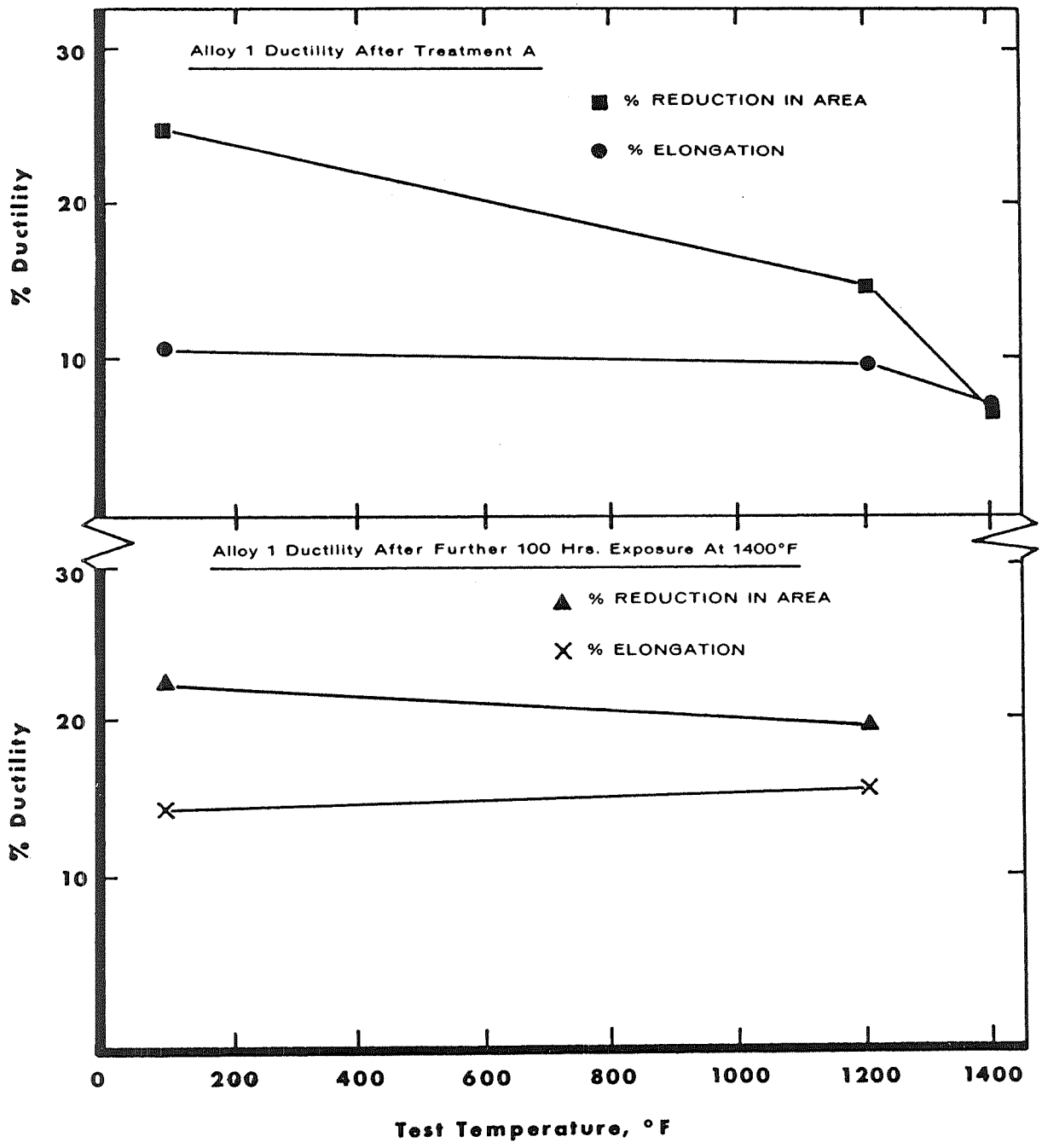
Alloy 1 Ductility After Treatment A
% REDUCTION IN AREA
% ELONGATION
% Ductility
30
20
10
Alloy 1 Ductility After Further 100 Hrs. Exposure At 1400°F
% REDUCTION IN AREA
% ELONGATION
% Ductility
30
20
10
0
200
400
600
800
1000
1200
1400
Test Temperature, °F

Fig. 13.

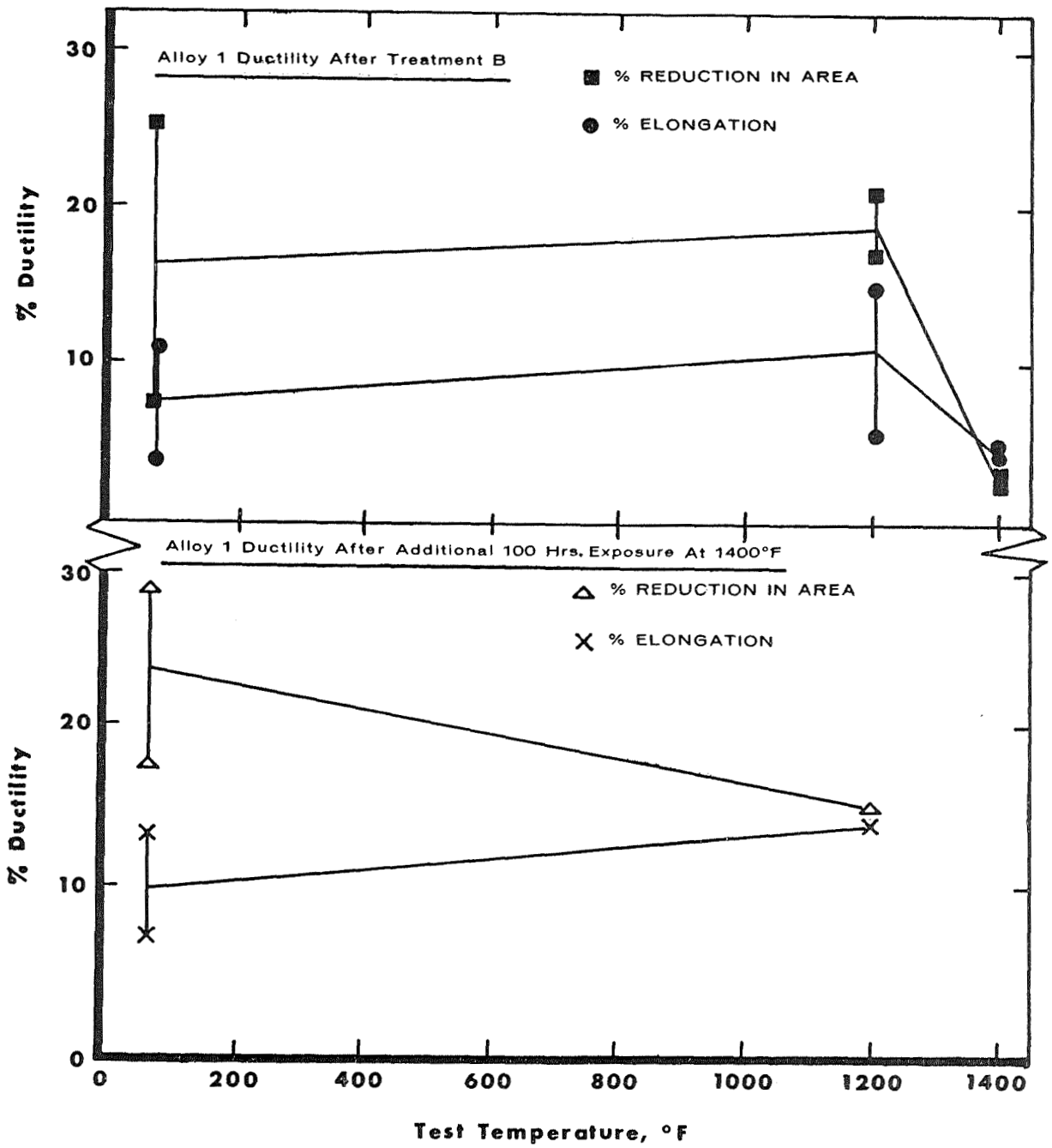
Alloy 1 Ductility After Treatment B
% REDUCTION IN AREA
% ELONGATION
% Ductility
30
20
10
Alloy 1 Ductility After Additional 100 Hrs. Exposure At 1400°F
% REDUCTION IN AREA
% ELONGATION
% Ductility
30
20
10
0
0
200
400
600
800
1000
1200
1400
Test Temperature, °F

Fig. 14.

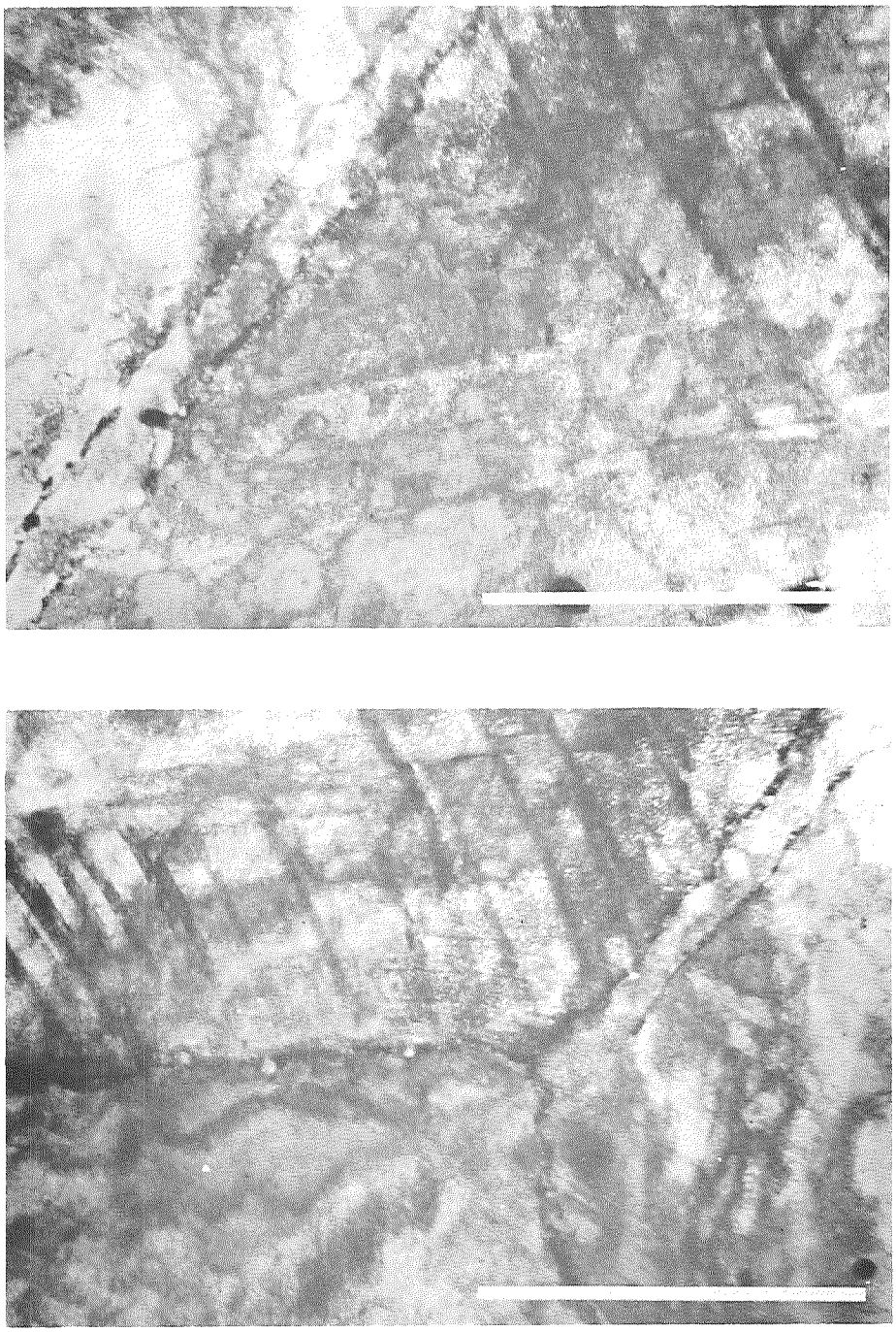

Figure 15. Thin foil micrographs taken from the cross section of the gauge length of an Alloy 1 tensile specimen tested at room temperature. Test No. 41211 The line marks on the micrographs represent one micron.

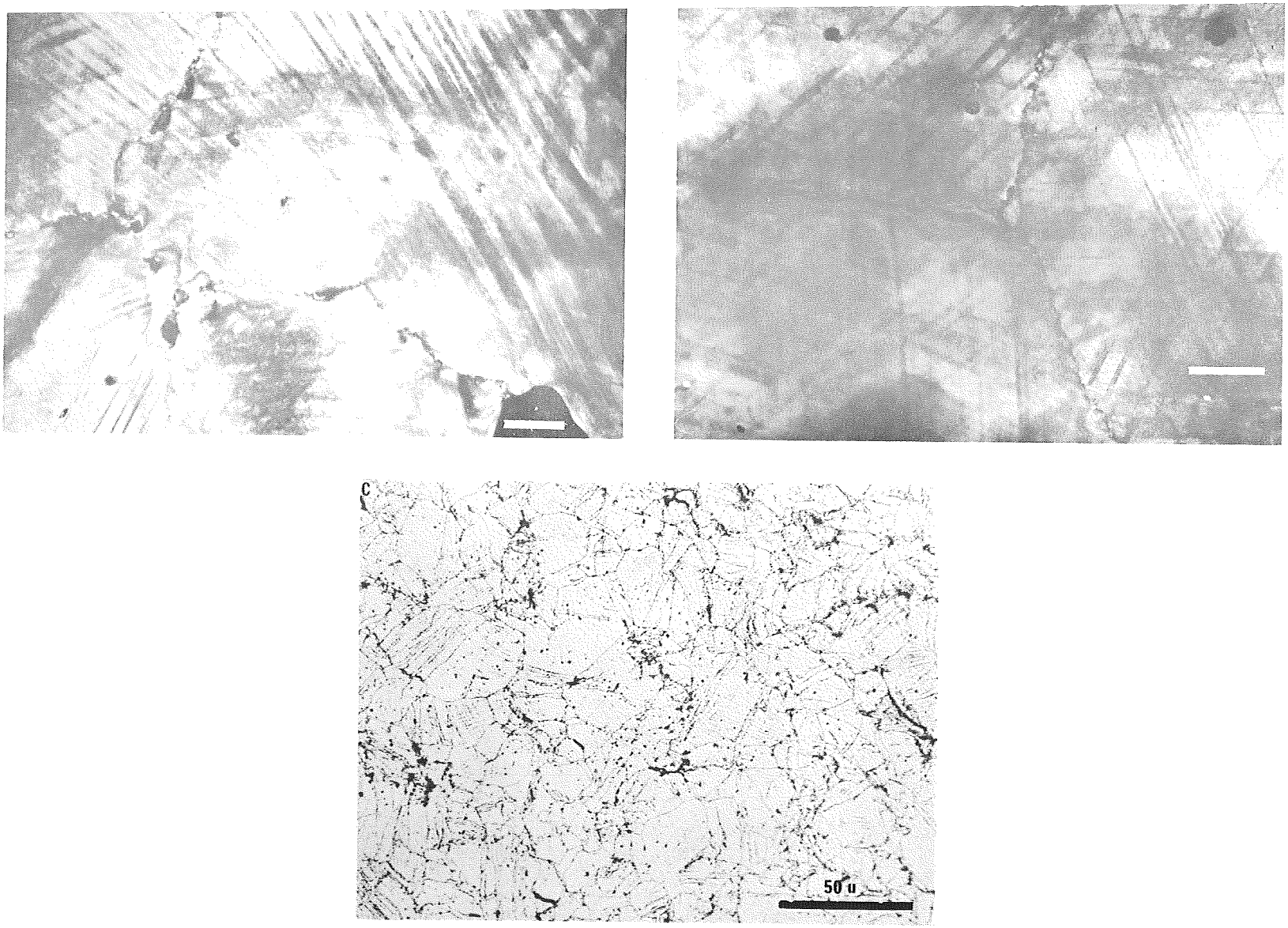

Figure 16. (A) and (B). Thin foil micrographs taken from the cross section of the gauge length of an Alloy 1 tensile specimen tested at 1200° F. Test No. 41213. The line marks on the micrographs represent one micron. (C) Optical micrograph of a cross section of Alloy 1 after tensile test at 1200° F.

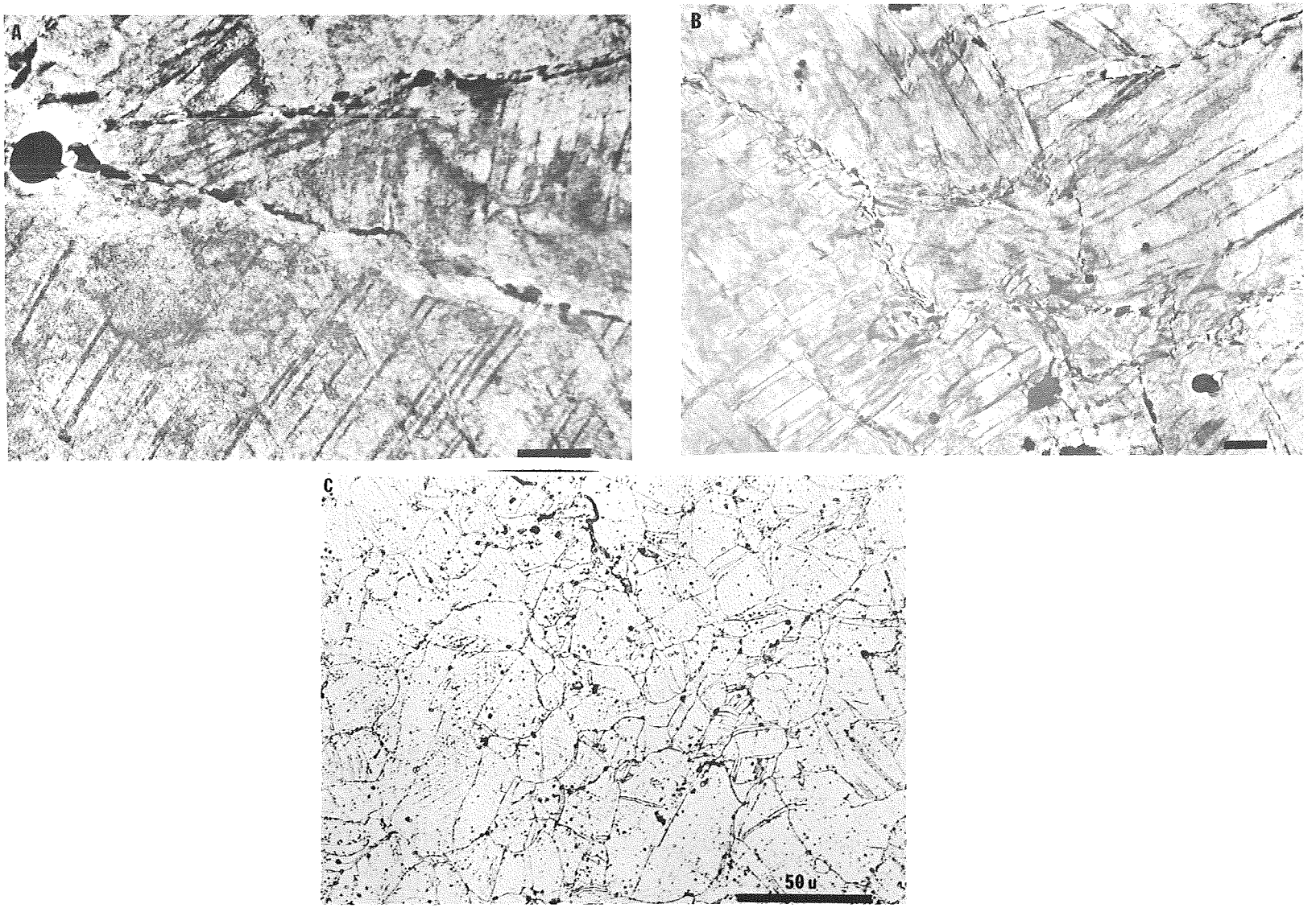

Figure 17. (A) and (B). Thin foil micrographs of a cross section of the gauge length of an Alloy 1 tensile specimen tested at 1400° F. Test No. 41216. The line marks on the micrographs represent one micron. (C) Optical micrograph of a cross section of Alloy 1 after tensile test at 1400° F.

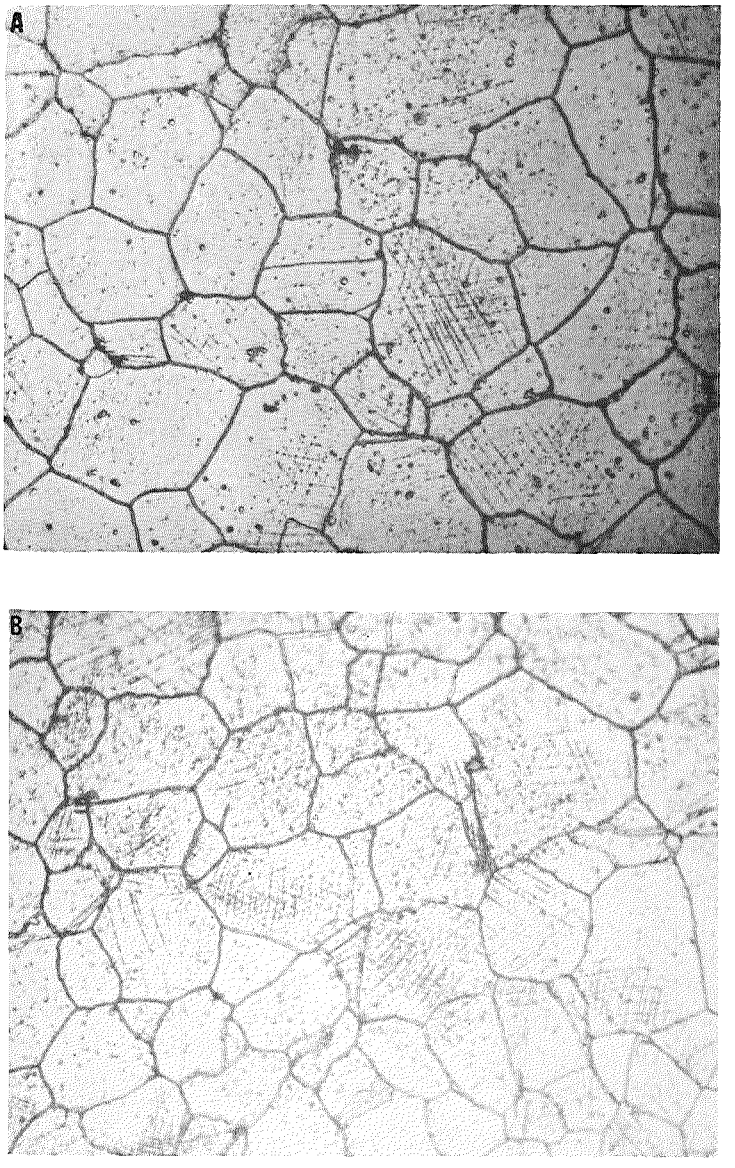

Figure 18. Optical micrographs of the cross section of stress rupture specimens (A) Alloy 1 tested in the "as-cold-swaged plus 120 hours at 1200° F " condition. Test parameters were 110,000 psi and 1200° F. Stress rupture life of 37.5 hours. Test No. 10,252. (B) Alloy 1 specimen tested in the "as-cold-swaged plus 120 hours at 1200° F" condition. Test parameters 150,000 psi at 1200° F. Stress rupture life 2.75 hours. Test No. 10,255. 500x.

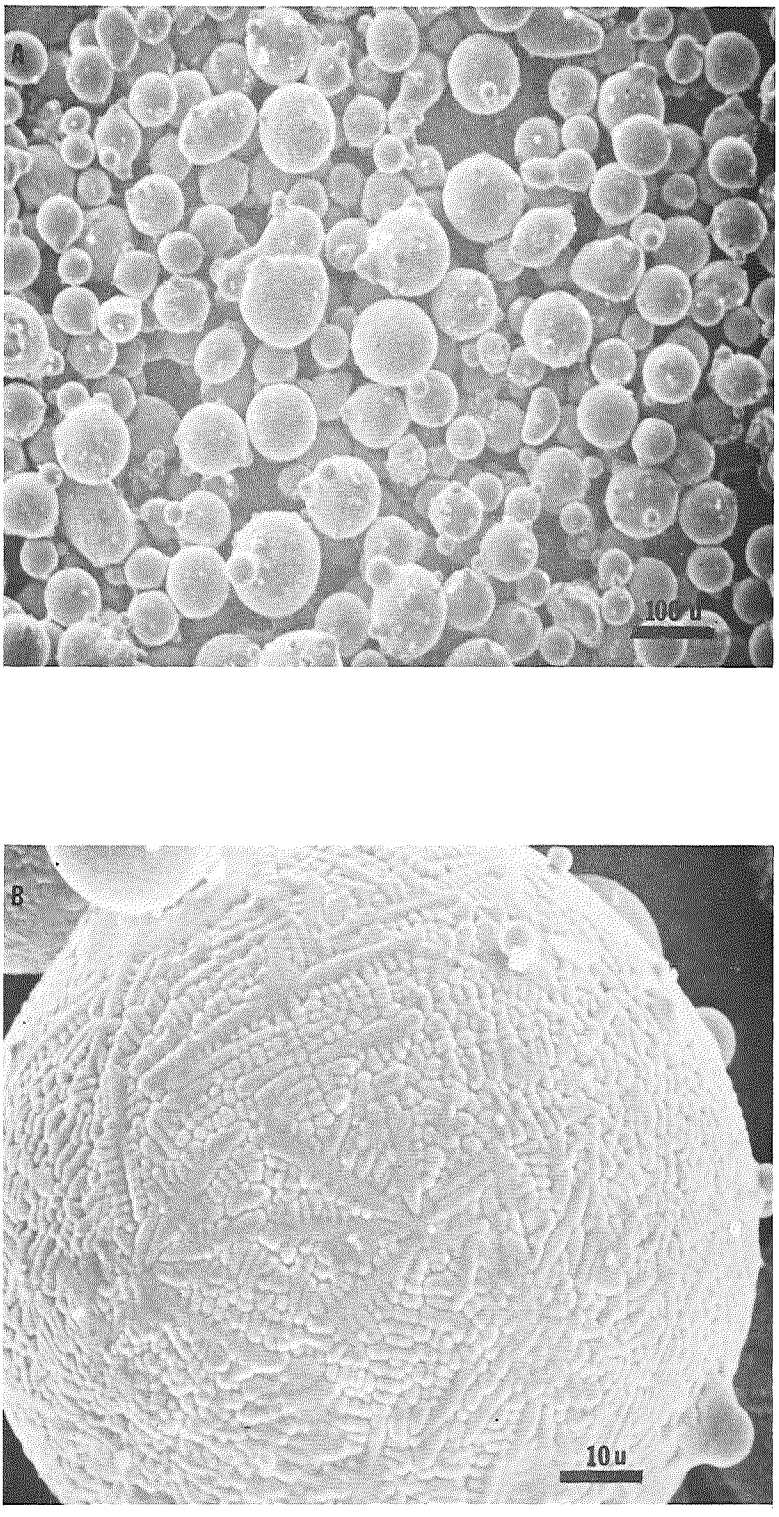

Figure 19. (A & B) Scanning electron micrographs of 100/325 mesh fractic of alloy 2 powders.

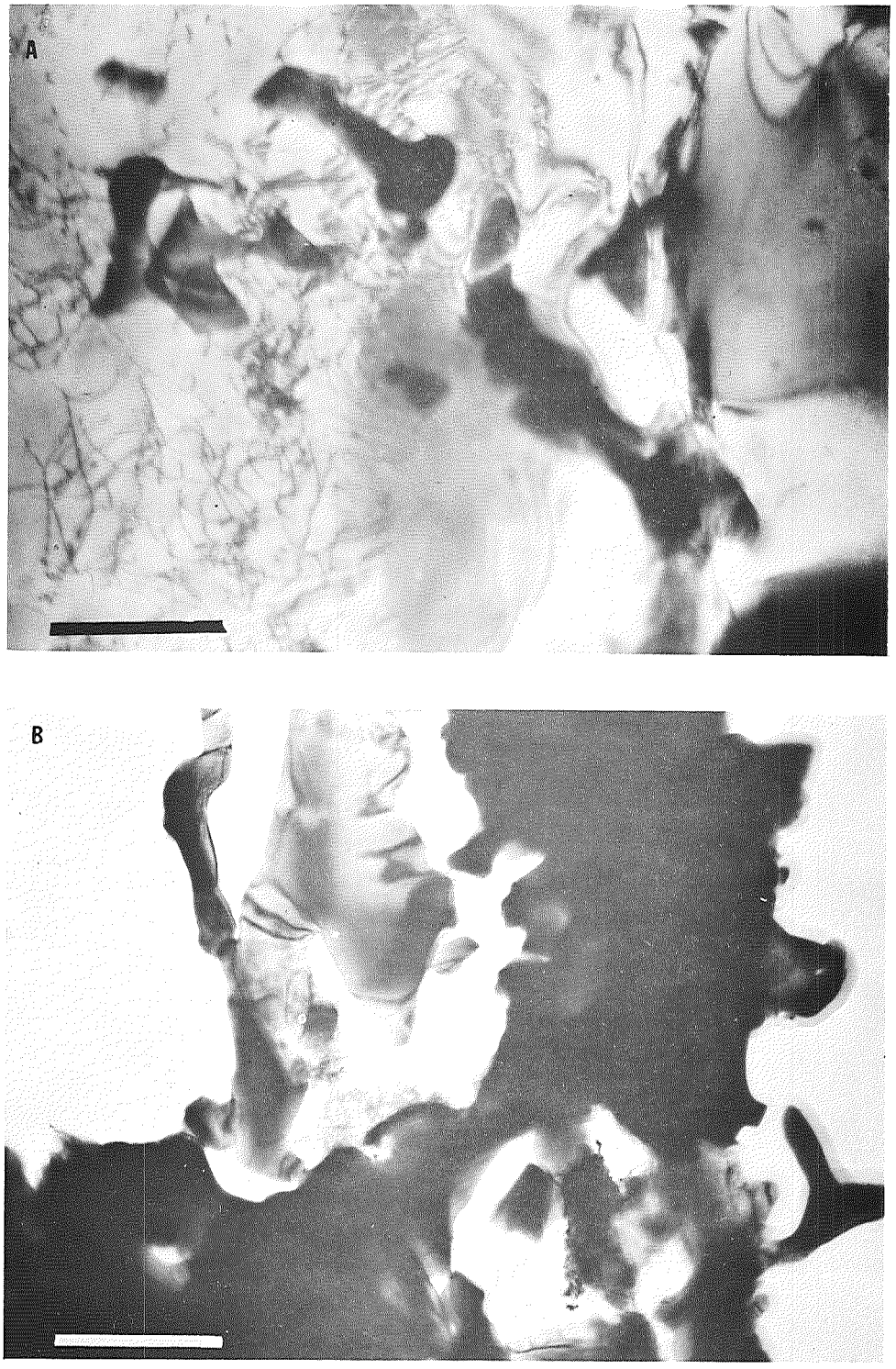

igure 20. Thin foil micrographs of individual particles of alloy 2 powders
se transmission micrographs have been prepared by "holding" the particles
lectrolytic nickel plate as shown in Figure 2). The line marks represent
nicron.

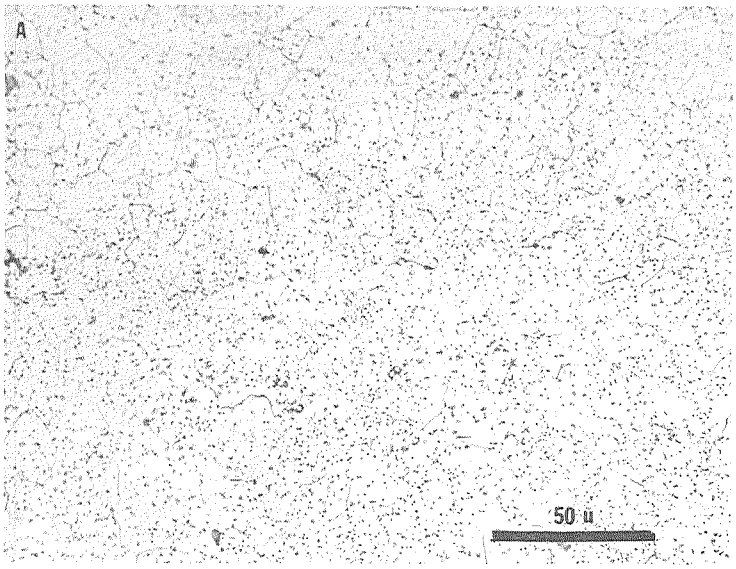

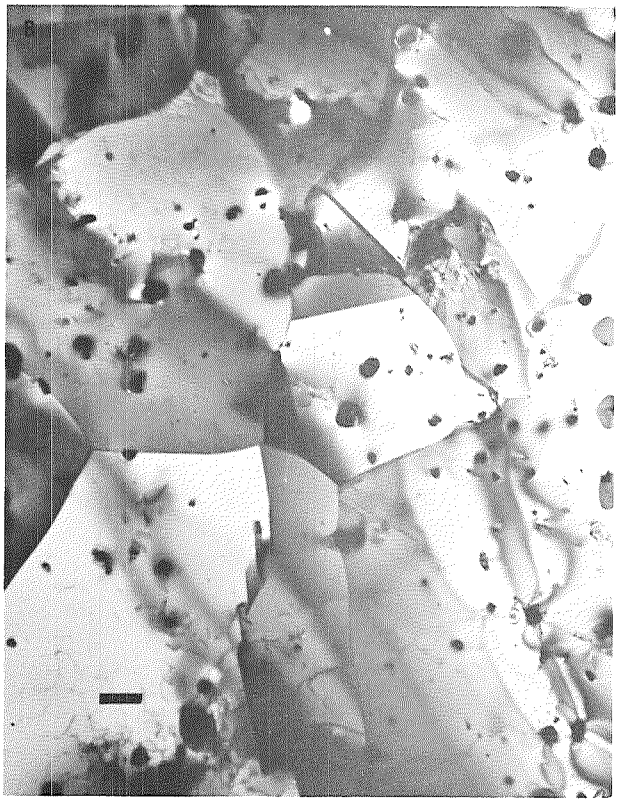

Figure 21. (A) Optical micrograph of as-extruded bar made by canning and extruding 100/325 mesh fraction of alloy 2 powder; (B & C) thin foil micrographs of the as-extruded material showing the finely distributed MC carbides. The line marks represent one micron.

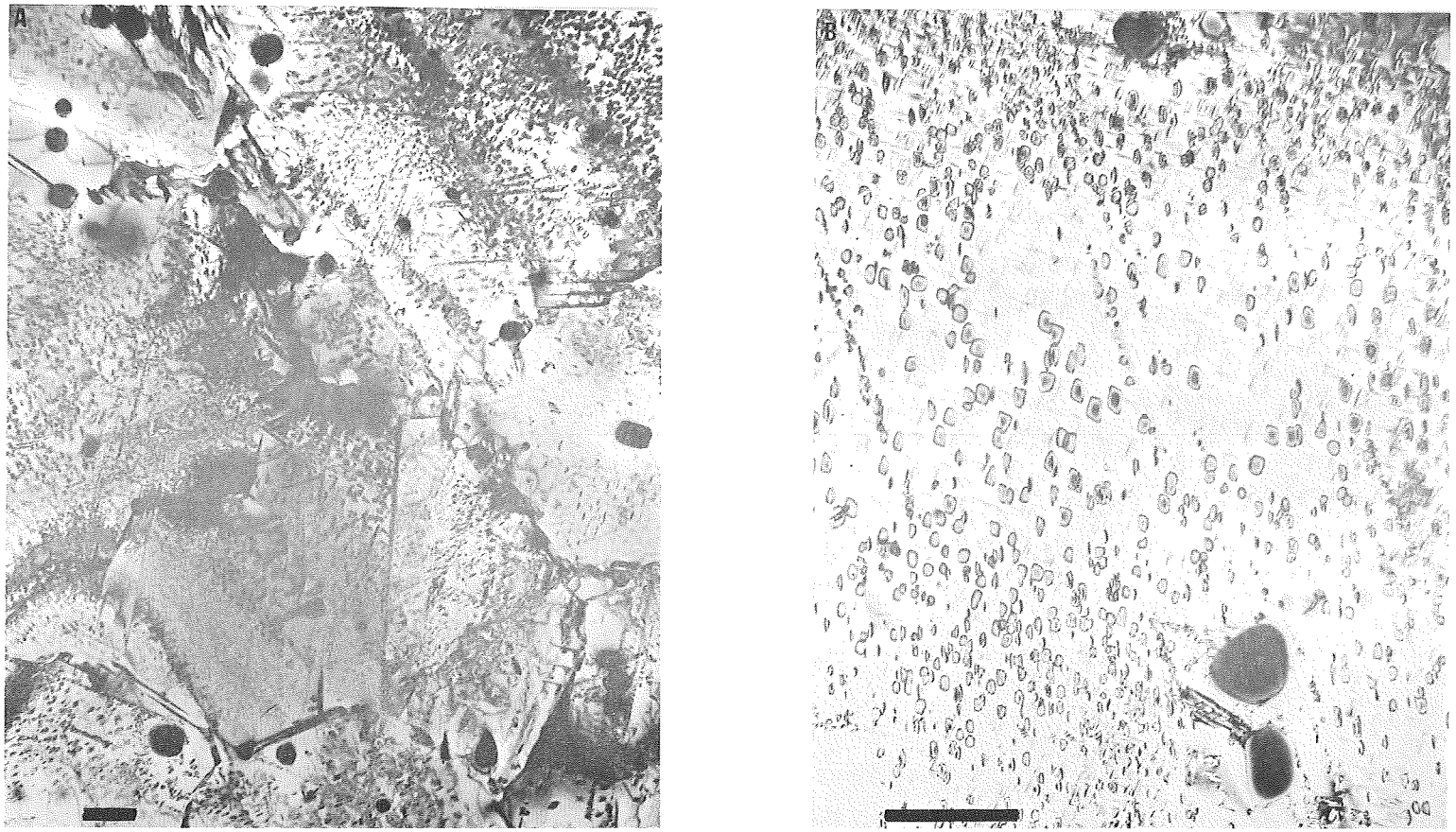

Figure 22. (A & B) Thin foil micrographs of as-extruded alloy 2 P/M bar aged for 8 hours at 1350°F. In (A) the overall microstructure of several grains can be seen and in (B) the morphology of the Ni_3Cb strengthening precipitate is shown. The line marks represent one micron.

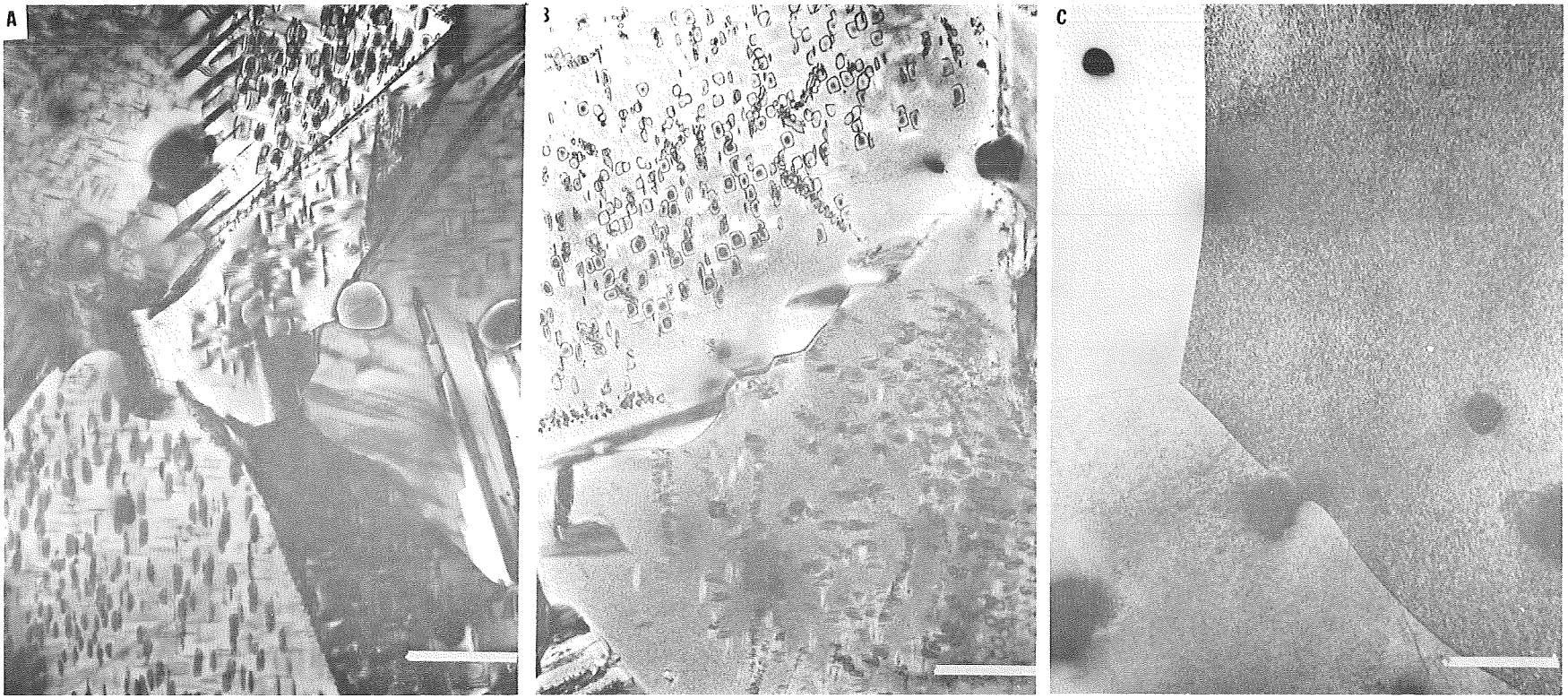

Figure 23. Thin foil micrographs of alloy 2 extruded bar after various heat treatments. (A) Aged for 24 hours at 1350°F; (B) aged for 8 hours at 1350°F plus 48 hours at 1150°F; and (C) aged for 51 hours at 1200°F. The line marks on each micrograph represent one micron.

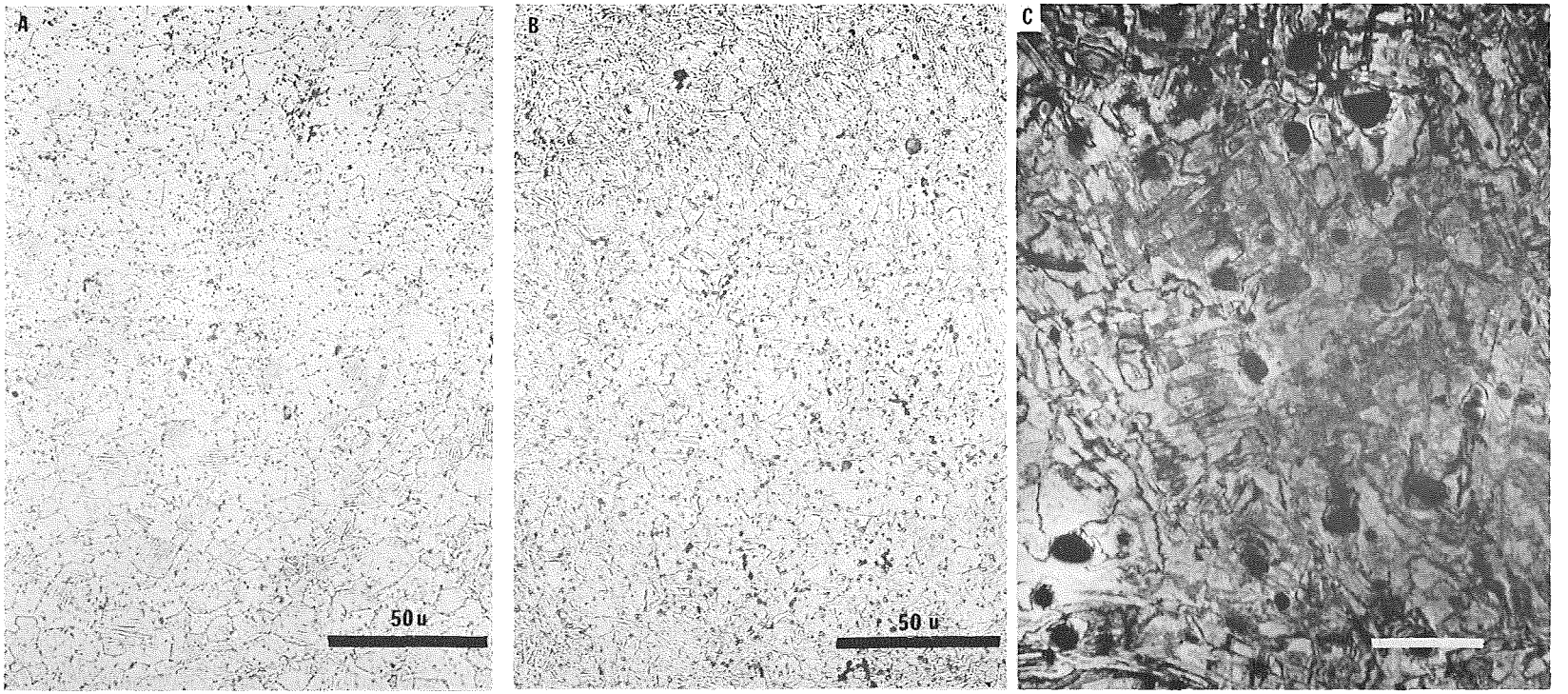

Figure 24. (A) Optical micrograph of alloy 2 P/M bar as-extruded and directly cold-swaged to 0.600" diameter; (B) optical micrograph of alloy 2 P/M bar cold-swaged as in (A) above, intermediate annealed for 8 minutes at 2200°F, quenched and further cold swaged to 0.495" diameter; and (C) thin foil transmission micrograph of the cold-swaged bar as in (B) above. Line mark represents one micron.

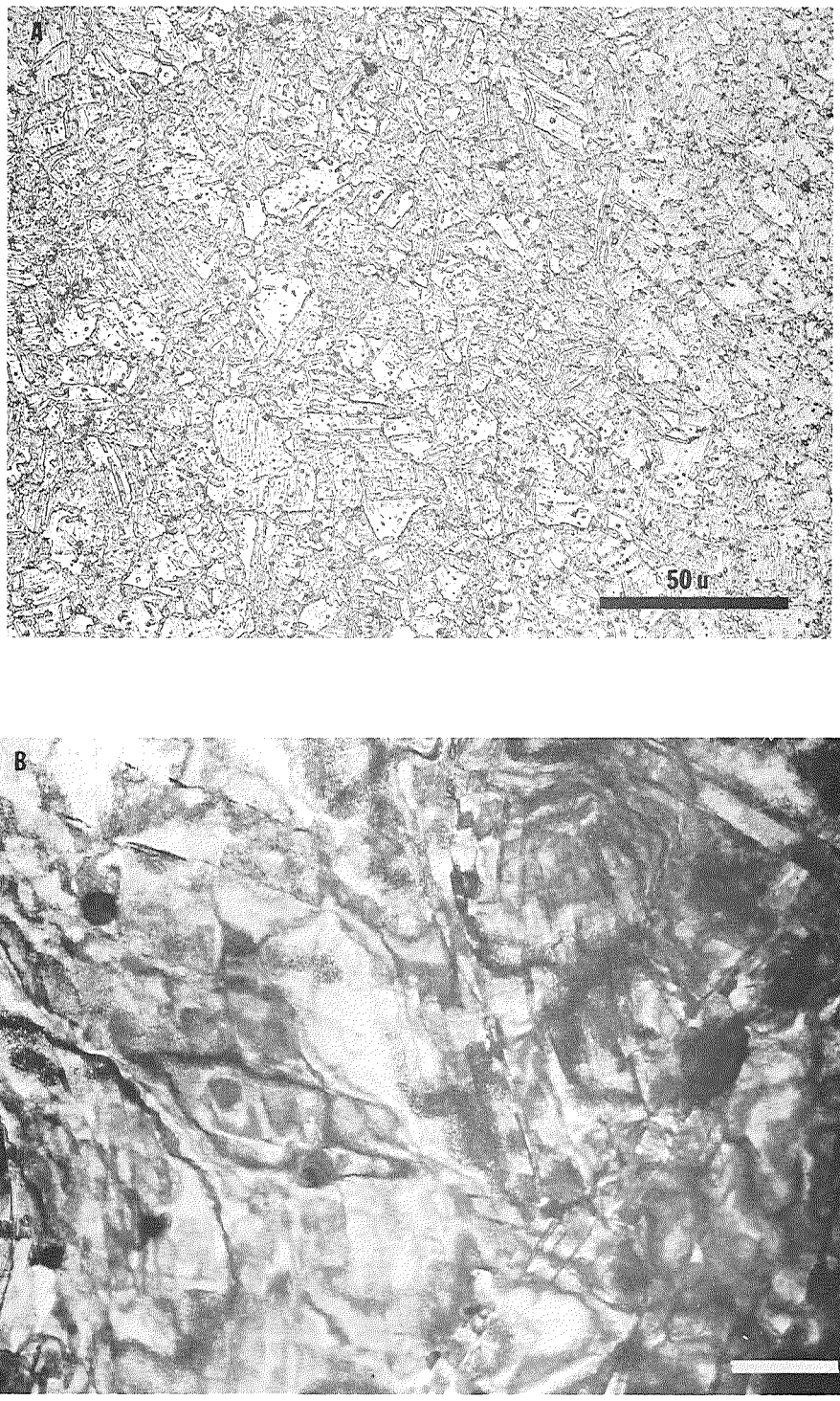

Figure 25. (A) Optical micrograph of alloy 2 P/M rod, cold-swaged to 0.495" diameter and aged for 120 hours at 1200°F; and (B) thin foil electron micrograph of alloy 2 P/M rod, cold-swaged to 0.495" diameter and aged for 120 hours at 1200°F. Line mark represents one micron.

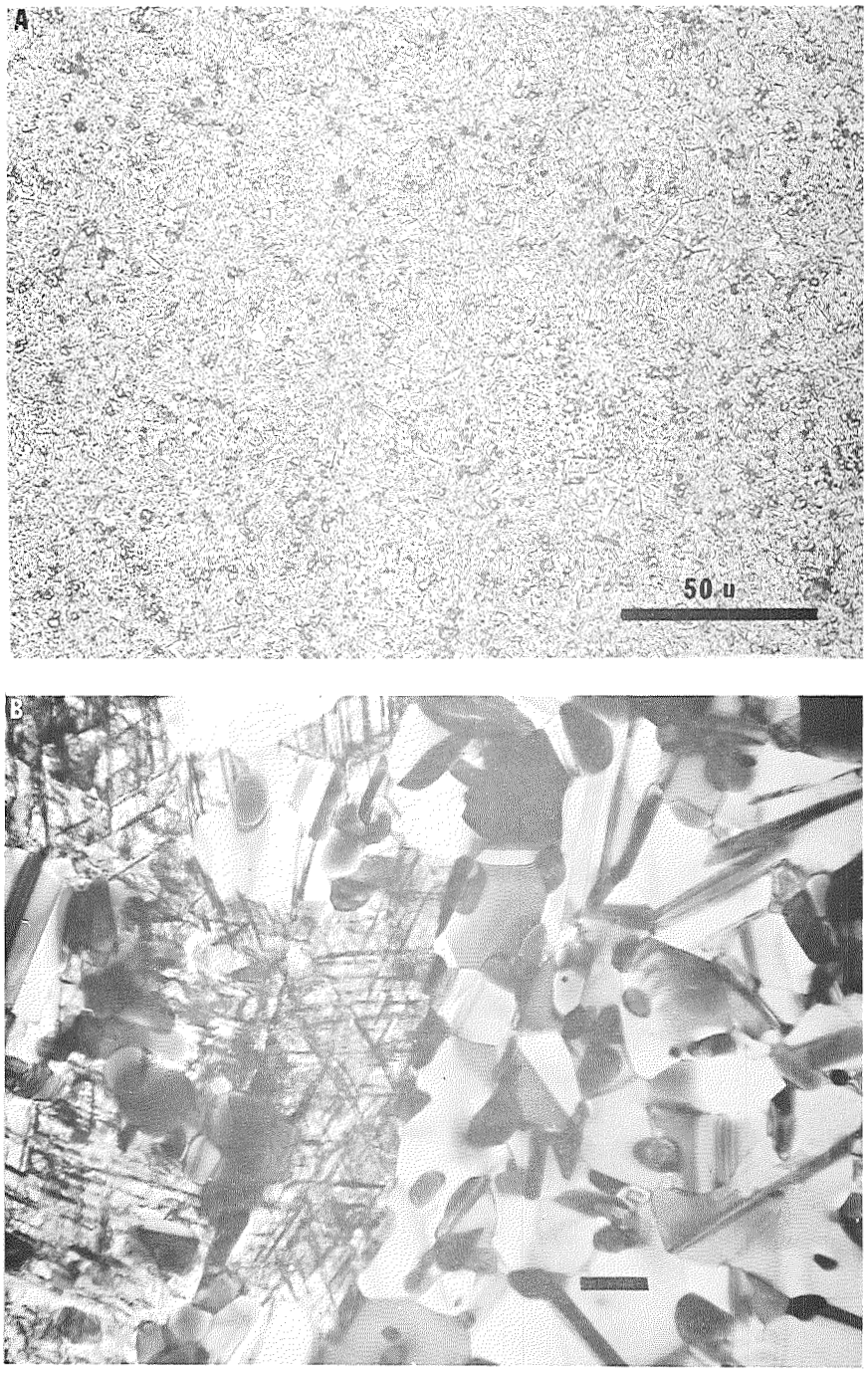

Figure 26. (A) Optical micrograph; and (B) thin foil micrograph of alloy 2 P/M rod, cold-swaged to 0.495" diameter, aged for 120 hours at 1200°F and further exposed for 100 hours at 1400°F. Line mark in (B) represents one micron.

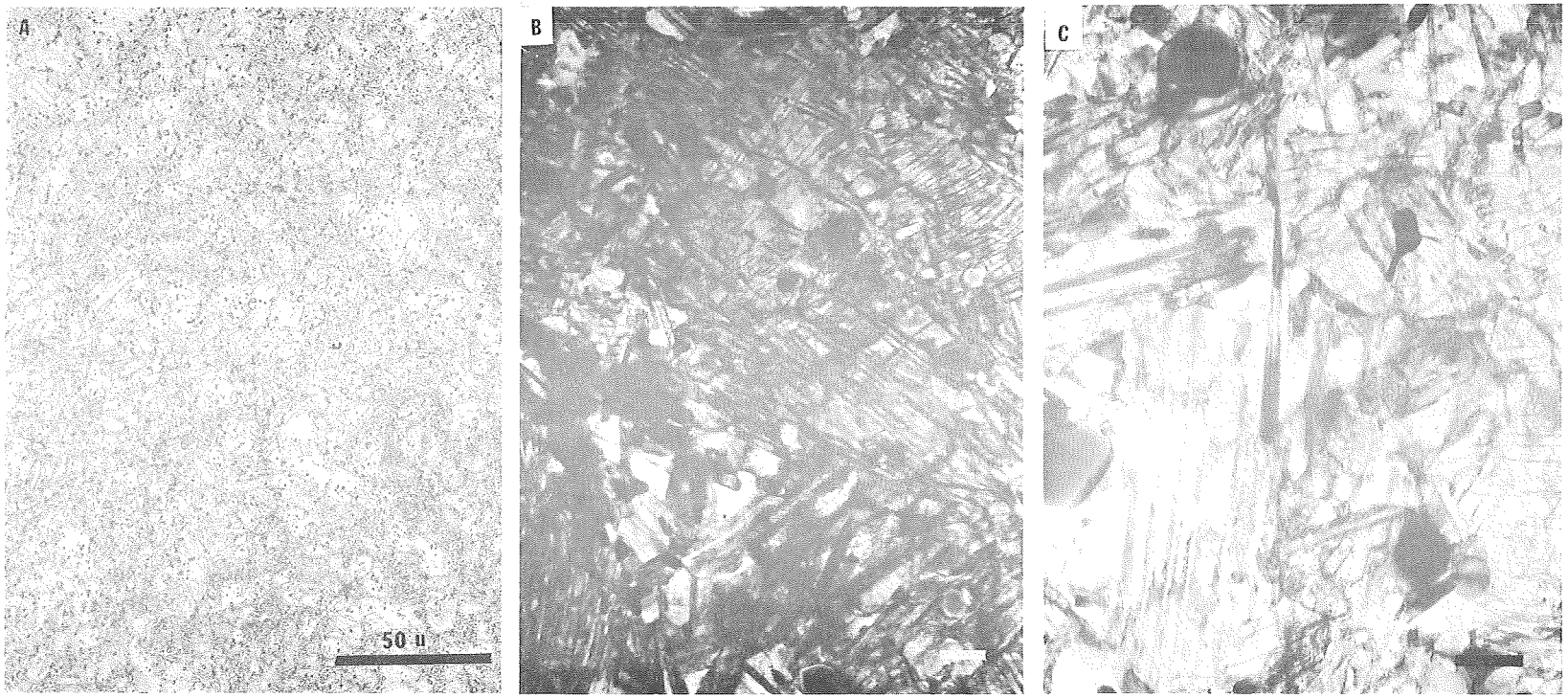

Figure 27. Microstructure of alloy 2 bar after room temperature tensile test. Test No. 43263. All micrographs are from a cross-section of the gauge length of the tensile specimens. Line marks on thin foil micrographs represent one micron. (A) Optical micrograph; (B) and (C) thin foil micrographs.

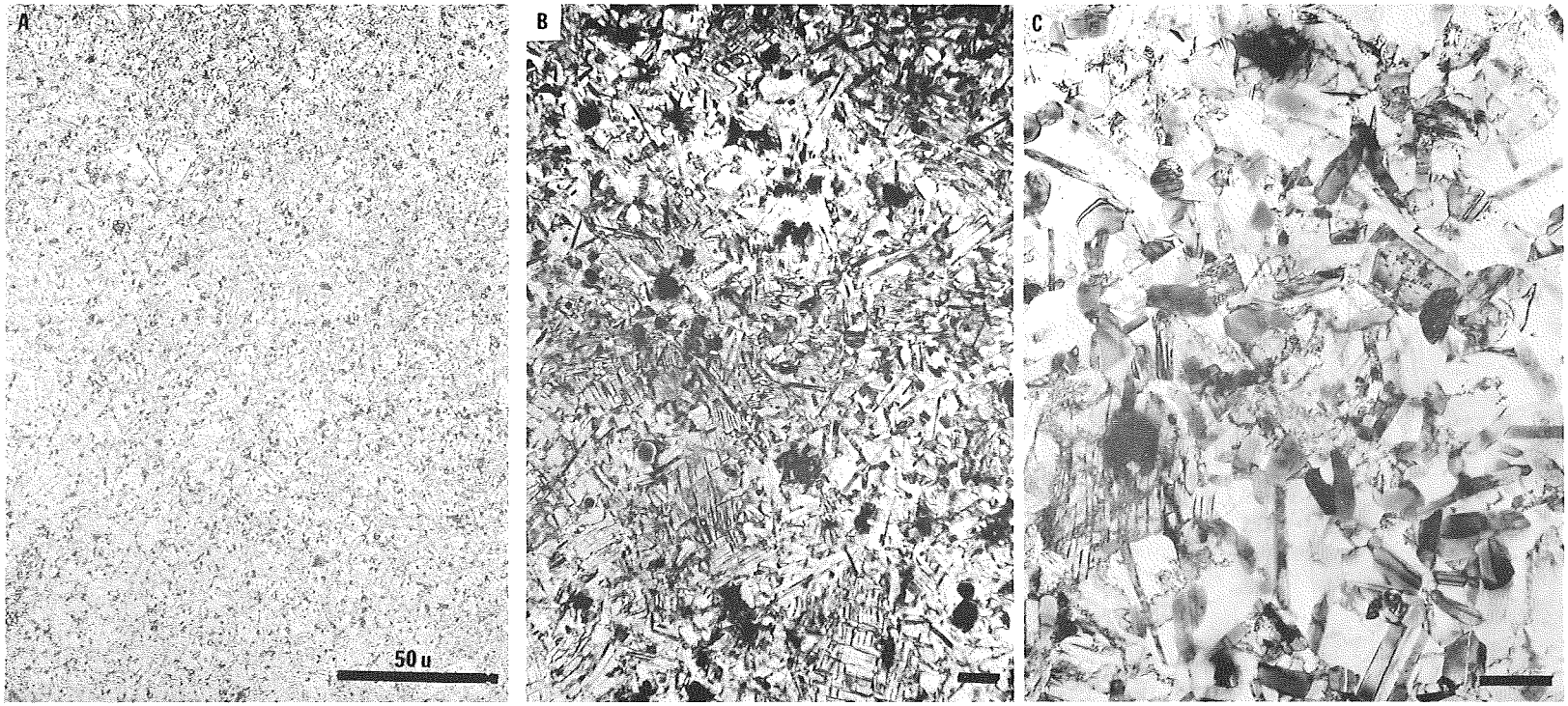

Figure 28. Microstructure of alloy 2 bar after 1200°F tensile test. Test No. 43266. All micrographs are from a cross-section of the gauge length of the tensile specimen. Line marks on thin foil micrographs represent one micron. (A) Optical micrograph; (B) and (C) thin foil micrographs.

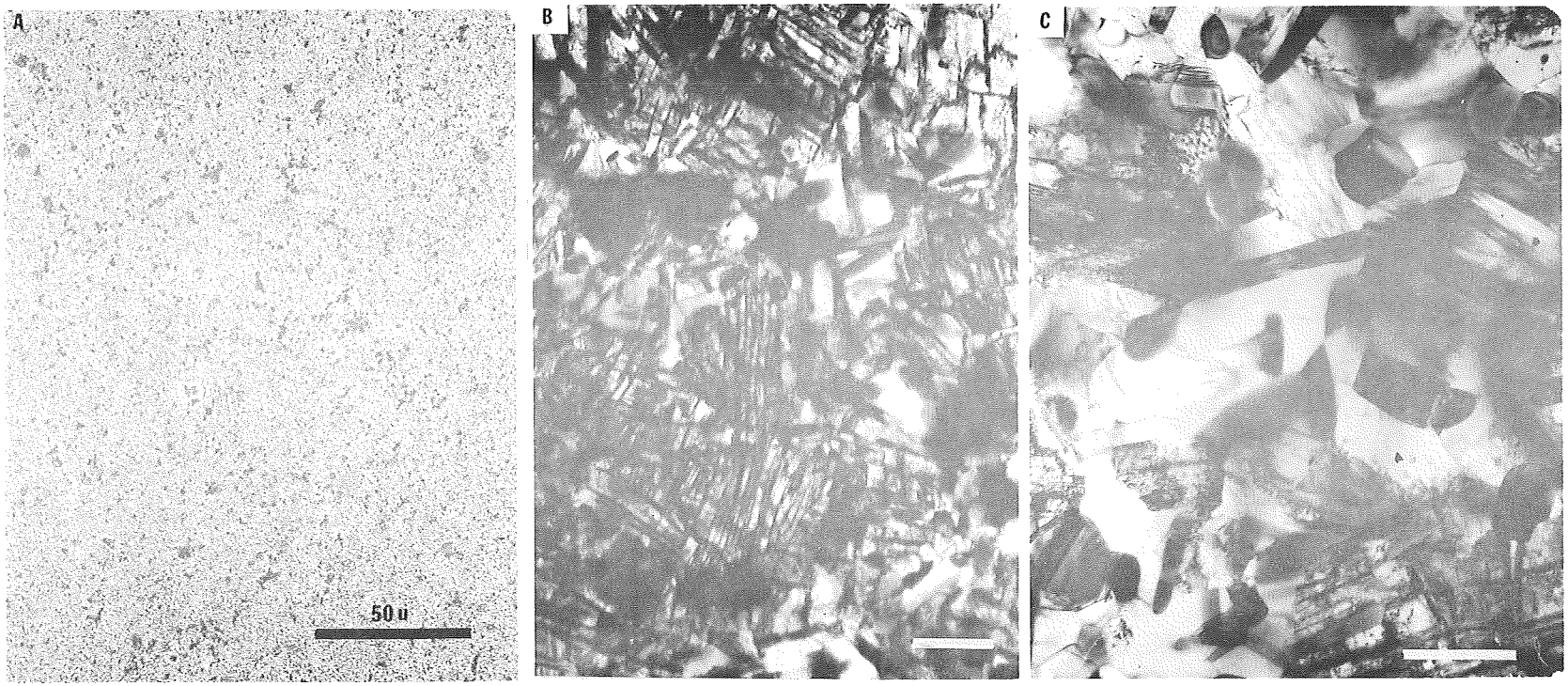

Figure 29. Microstructure of alloy 2 bar after 1400° F tensile test. Test No. 43268. All micrographs are from a cross-section of the gauge length of the tensile specimen. Line marks on thin foil micrographs represent one micron. (A) Optical micrograph; (B) and (C) thin foil micrographs.

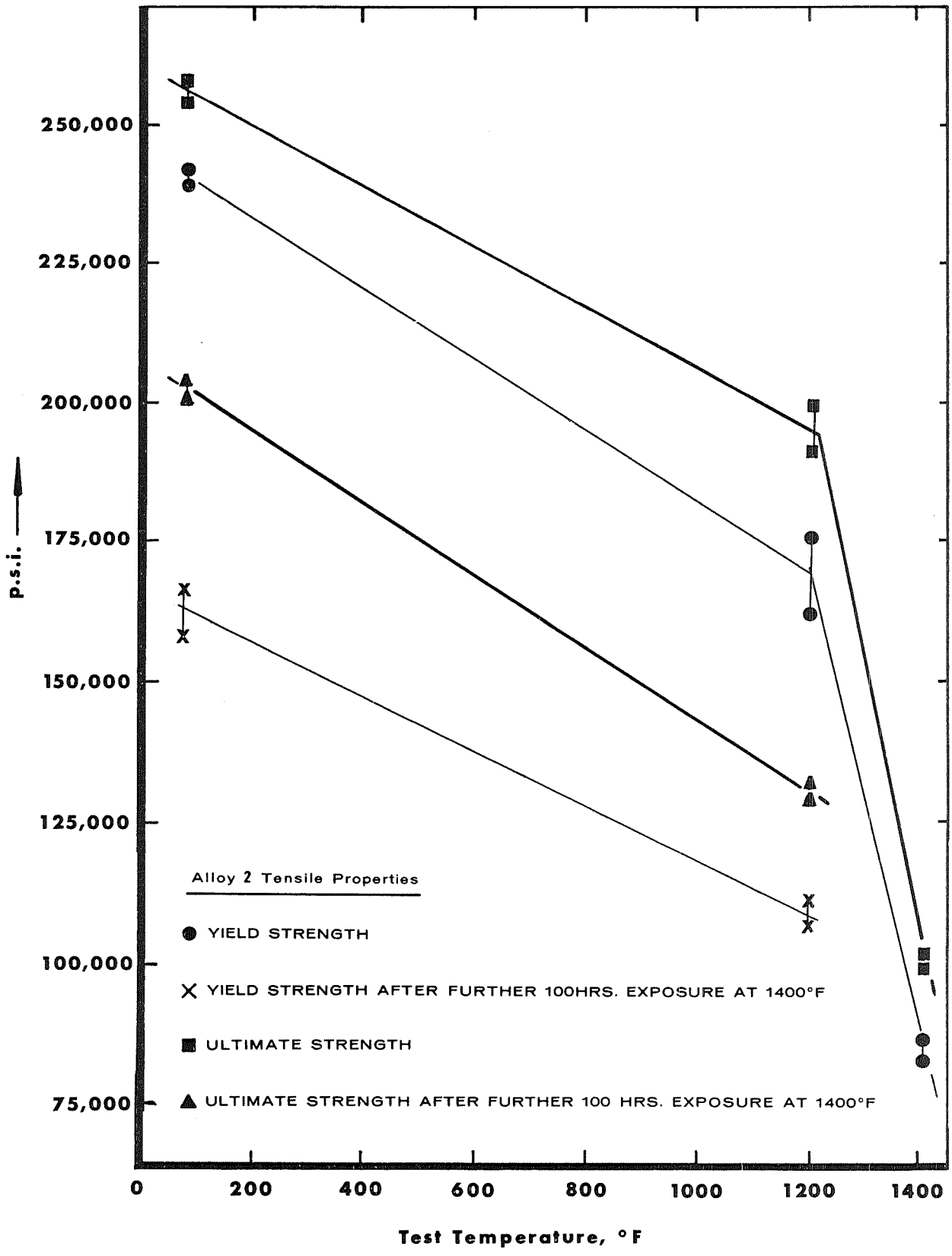
250,000
225,000
200,000
175,000
150,000
125,000
100,000
75,000
p.s.i.
Alloy 2 Tensile Properties
YIELD STRENGTH
YIELD STRENGTH AFTER FURTHER 100HRS. EXPOSURE AT 1400°F
ULTIMATE STRENGTH
ULTIMATE STRENGTH AFTER FURTHER 100 HRS. EXPOSURE AT 1400°F
0
200
400
600
800
1000
1200
1400
Test Temperature, °F

Fig. 30

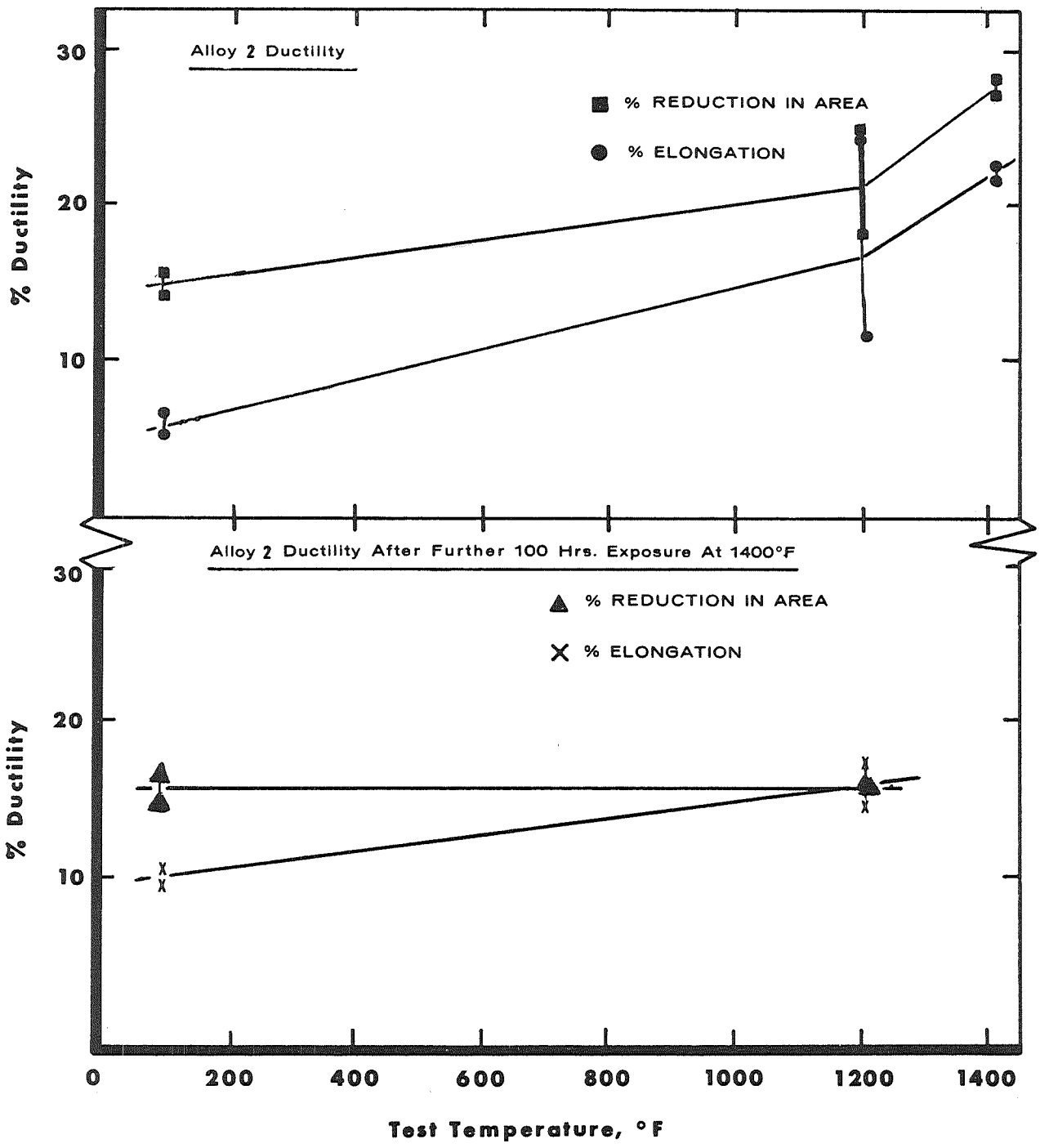
Alloy 2 Ductility
% REDUCTION IN AREA
% ELONGATION
% Ductility
30
20
10
Alloy 2 Ductility After Further 100 Hrs. Exposure At 1400°F
% REDUCTION IN AREA
% ELONGATION
% Ductility
30
20
10
0
200
400
600
800
1000
1200
1400
Test Temperature, °F

Fig. 31

APPENDIX A

In this Appendix, data (extrinsic to the present contract) is presented on the coarsening behavior of the Ni_3Ta precipitate in a wrought (conventionally processed) superalloy, similar to Alloy 1, of the following composition:

Ni - 20.47 Cr - 5.59 Fe - 5.41 Mo - 9.82 Ta - 5.02 Co - .089 C

Samples of this alloy were solution heat-treated at 2282°F (1250°C) quenched and aged at 1200°F (650°C), 1300°F (705°C), 1400°F (760°C) and 1500°F (815°C). The morphology of the Ni_3Ta b.c.tetragonal precipitate after 25 hours and 100 hours at the above temperatures is shown in the successive thin foil micrographs in Figure A. An increase in size of the Ni_3Ta b.c.tetragonal precipitates can be observed as the aging temperature is increased from 1200°F (650°C) to 1500°F (815°C). It is worth noticing that the large Ni_3Ta precipitates observed after 100 hours at 1500°F (815°C) are still coherent as is manifested by the existence of delta fringes at the precipitate/matrix interface. Unlike the situation in the case of the deformed matrix in Alloy 1 (where the commencement of recrystallization after 100 hours at 1400°F (760°C) is accompanied by a transformation from b.c.tetragonal Ni_3Ta to orthorhombic Ni_3Ta), in the present case no transformation of the Ni_3Ta b.c.tetragonal precipitate occurs.

Figure B is a log-log plot of half the Ni_3Ta platelet length (a/2) against hours of aging time for three temperatures. The lengths of the platelets for each heat treatments were measured for micrographs where the foil orientation resulted in the platelets being "edge-on". As shown in Figure B the log a/2 vs log t (time) plots show a slope of 1/2. Assuming a relation of the type:

$$a/2 = K \cdot t^n$$

where K is the rate constant for a particular aging temperature, n is determined to be 1/2. Following from this, in Figure C, a/2 is plotted against $t^{1/2}$ and a linear fit is obtained. The rate constants, K, for each aging temperature can now be determined either from the intercepts of the log a/2 vs log t curves with the y axis at t = 1 in Figure B or from the slopes of the a/2 vs $t^{1/2}$ plots in Figure C.

In Figure D, log K (K being the rate constants for each aging temperature) calculated from Figures B and C) is plotted against the reciprocal of aging temperature in °K. From this plot a value of activation energy for growth of the Ni_3Ta b.c.tetragonal precipitate is obtained. The activation energy is calculated to be 51.5 K Cals/mole. (Tutunik and Estoulin[5] have calculated the activation energy for diffusion of Ta in Ni to be 57 K Cals/mole.)

From the foregoing it would appear that the same precipitate growth process occurs at all of the aging temperatures investigated and that no transformation of the b.c.tetragonal Ni_3Ta precipitate occurs for aging treatments up to 100 hours at 1500°F (815°C).

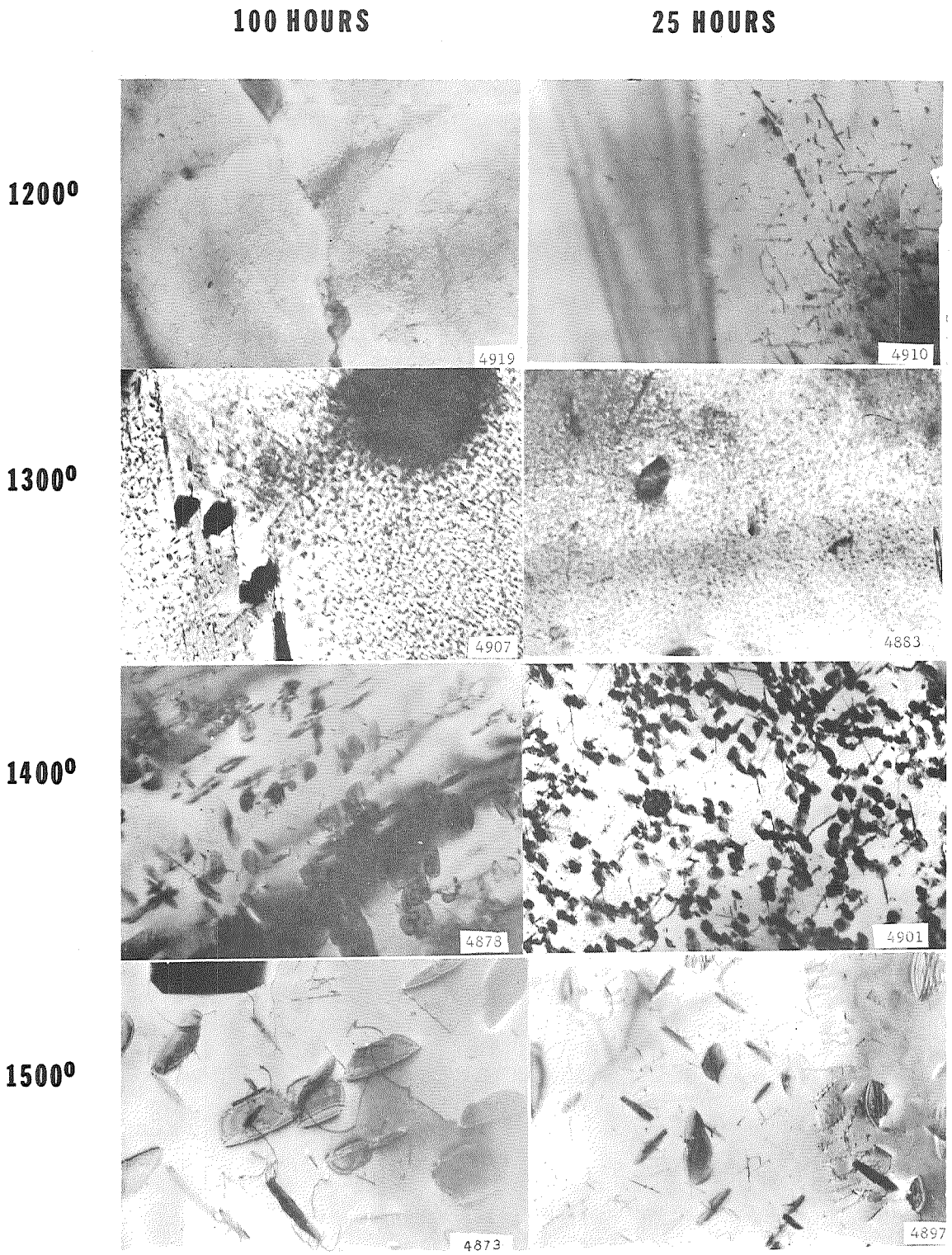

Figure A (Appendix A)

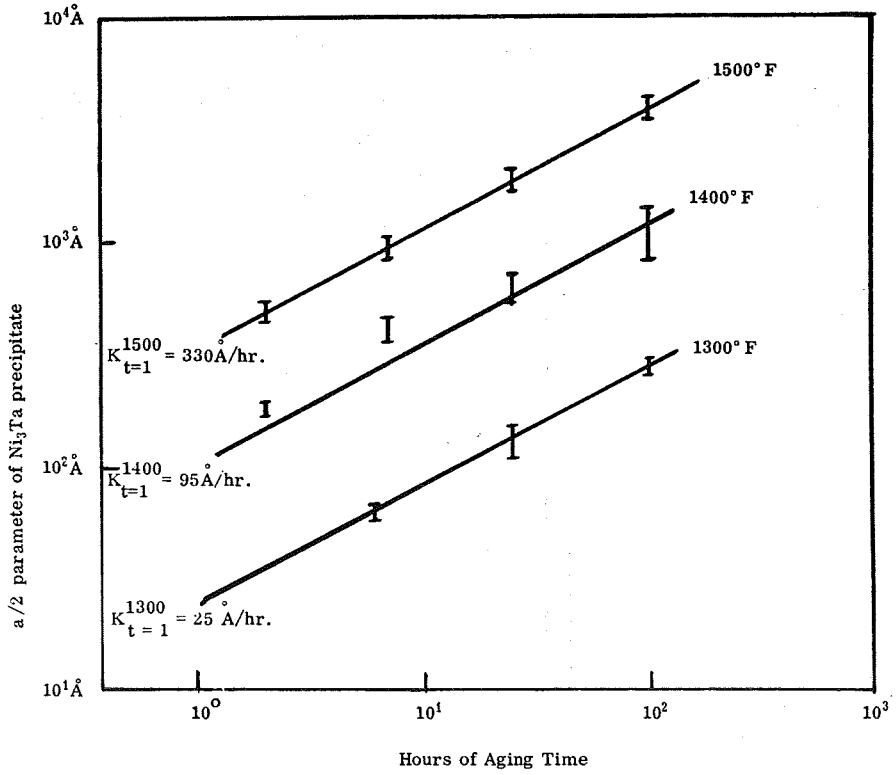

Figure B. Log-log plot of a/2 versus aging time in hours. The intercept at unit time gives a measure of the Rate Constant at three temperatures. Slope of all the a/2 versus t curves is 1/2.

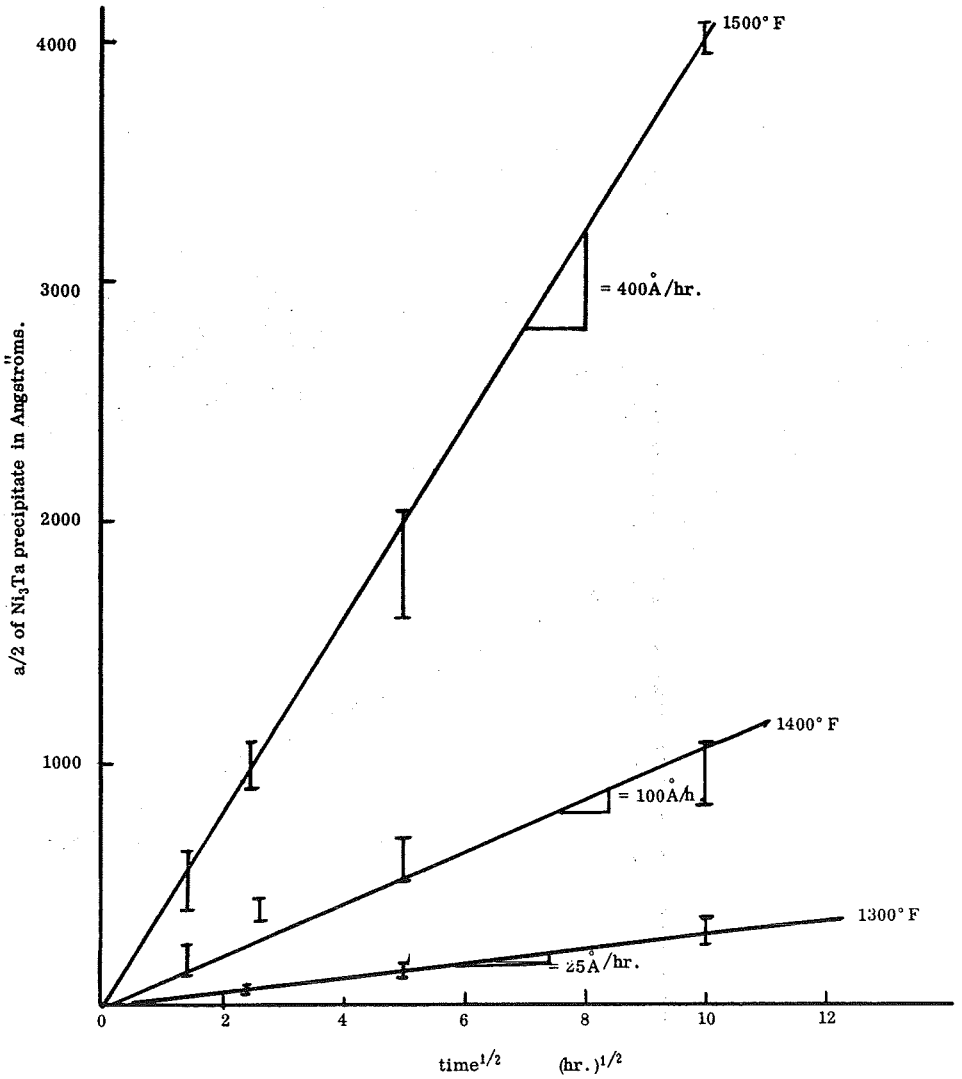

Figure C. Plot of a/2 versus $t^{1/2}$ at three temperatures for Ni_3Ta precipitate.

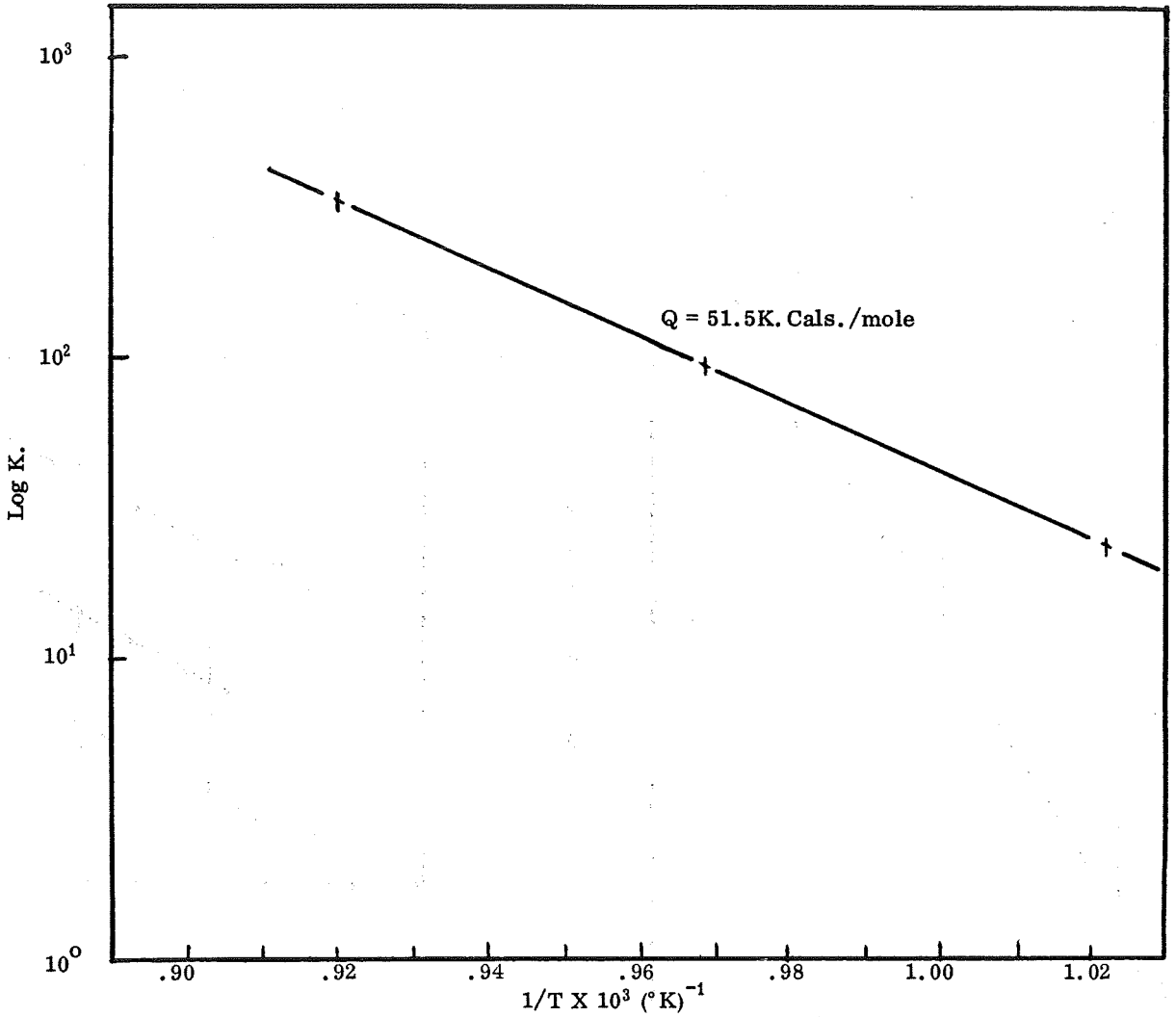

Figure D. Plot of Log K versus $^{1}/_{T}$ in °K for three temperatures of aging.

APPENDIX B

In this Appendix, X-ray diffraction data on phases extracted from Alloy 1 is presented. The extracted phases are representative of Alloy 1 in two conditions:

A. As cold-swaged and aged for 120 hours at 1200°F (650°C)

B. As cold-swaged, aged for 120 hours at 1200°F (650°C) plus further aged for 100 hours at 1400°F (760°C)

The diffraction data is presented to show that after 100 hours at 1400°F (760°C), there occurred a transformation of the b.c.tetragonal Ni_3Ta phase to orthorhombic Ni_3Ta phase. This transformation accompanies the recrystallization observed after the 100 hours exposure at 1400°F (760°C). (See Figures 9a thru d.) Without a cold-worked matrix, no formation of Ni_3Ta orthorhombic phase occurs even after exposure for 100 hours or more at 1500°F (815°C). The d spacings from the X-ray data are presented on the next page.

X-RAY DIFFRACTION DATA FROM PHASES EXTRACTED FROM ALLOY 1 SPECIMENS

A = 120 Hrs. at 1200°F (650°C)

B = 120 Hrs. at 1200°F (650°C) + 100 Hrs. at 1400°F (760°C)

d Spacings A	d Spacings B	Ni_3Ta b.c.Tet.	Ni_3Ta Ortho.	MC TaC Type	$M_{23}C_6$	FCC Matrix
	4.418					
	4.124					
4.104						
	3.731	(002)				
	3.534					
	3.339		(101)			
3.283						
	3.243	(101)	(110)			
	3.048		(011)			
	2.993					
	2.618		(111)			
2.545	2.539	(110)	(200)	(111)		
2.507						
2.382	2.380				(420)	
2.317	2.309					
2.206	2.201		(201)	(200)		
2.178	2.178				(422)	
	2.132					
	2.094	(112)	(020)			
2.064	2.053	(103)			(333)	(111)
1.995						
	1.965		(012)			
1.954	1.949		(211)			
1.884	1.884	(004)			(440)	
1.862						
	1.848					
	1.801	(200)			(531)	
1.789	1.783		(121)		(531)	(200)
1.706	1.707				(620)	
1.637	1.637	(202)				
1.601	1.610		(220)		(622)	
1.565	1.566	(211)	(310)	(220)		
	1.521	(114)	(221)			
1.500						
1.472						
	1.464		(122)			
1.376						
1.367						
	1.352	(213)				

d Spacings A	d Spacings B	Ni_3Ta b.c.Tet.	Ni_3Ta Ortho.	MC TaC Type	$M_{23}C_6$	FCC Matrix
1.335	1.336			(311)		
1.310						
1.285	1.295	(204)	(203)		(644)	
1.277						(220)
1.267	1.269	(220)	(400)	(222)	(660)	
1.262						
1.233	1.233	(006)			(555)	
	1.215	(222)				
1.186	1.184	(301)	(231)		(753)	
	1.136	(310)				
1.110	1.118	(116)	(004)			
1.092	1.098	(215,312)	(223)	(400)	(844)	
	1.087					
1.082	1.083		(420)		(933)	(311)
	1.069					
1.055	1.051	(224)				
1.036						(222)
1.017	1.016	(206,107)		(331)		
	1.001					
.991	.992	(321)			(1040)	
	.978	(314)				
	.968					
	.949					

REFERENCES

1. C. S. Kortovich, "Close Tolerance Forgings from P/M Preforms," AFML-TR-69-181, TRW Inc., June 1969.

2. K. H. Moyer, Final Report under Contract AF33(615)-3994, February 1969.

3. G. I. Friedman and P. Loewenstein, "Development of Processing Techniques for the Extrusion of Metal Powders", Whittaker Corporation, Nuclear Metals Division, December 1967.

4. P. S. Kotval, J. S. Dickey and B. E. Lewis, Proceedings of the 27th Annual Meeting of EMSA, 1969, p. 32.

5. A. D. Tutunnik and G. E. Estoulin, Fiz. Metal Metalloved (S.S.S.R), 1957, 4(3), p. 558.

DISTRIBUTION LIST FOR CONTRACT NAS3-13214

NASA Headquarters
600 Independence Avenue
Washington, D. C. 20546
Attn: G. C. Deutsch/RRM 1
R. H. Raring/RRM 1
J. Gangler/RRM 1
N. Rekos/RAP 1

NASA Lewis Research Center
21000 Brookpark Road
Cleveland, Ohio 44135
Attn: G. M. Ault, MS 105-1 1
N. T. Saunders, MS 105-1 1
A. E. Anglin, MS 106-1 1
F. H. Harf, MS 106-1 5
C. Blankenship, MS 105-1 1
R. L. Ashbrook, MS 49-1 1
J. W. Weeton, MS 49-1 1
J. C. Freche, MS 49-1 1
Aeronautics Procurement Section, MS 77-3 1
Library, MS 60-3 2
Patent Counsel, MS 500-311 1
Report Control Office, MS 5-5 1
W. J. Waters, MS 49-1 1
Technology Utilization Office, MS 3-19 1

NASA Scientific and Technical Information Facility
P. O. Box 3300
College Park, Maryland 20740
Attn: NASA Rep. RQT-2448 6

NASA Langley Research Center
Langley Field, Virginia 23365
Attn: Library 1
R. Pride, 188A 1

NASA Marshall Space Flight Center
Huntsville, Alabama 35812
Attn: Library 1

Jet Propulsion Laboratory
4800 Oak Grove Drive
Pasadena, California 91102
Attn: Library 1

NASA Ames Research Center
Moffett Field, California 94035
Attn: Library 1

NASA Goddard Space Flight Center
Greenbelt, Maryland 20771
Attn: Library 1

NASA Manned Space Flight Center
Houston, Texas 77058
Attn: Library 1

NASA Flight Research Center
P. O. Box 273
Edwards, California 93523
Attn: Library 1

FAA Headquarters
890 Independence Avenue, SW
Washington, D. C. 20553
Attn: Brig. Gen. J. C. Maxwell 1
F. B. Howard, SS-210 1
A. K. Forney 1

Headquarters
Wright Patterson AFB, Ohio 45433
Attn: MAG/A. M. Lovelace 1
MAM/H. M. Burte 1
MAAM/Technical Library 1
MAMS/C. T. Lynch 1
MAMP/I. Perlmutter 1
MAMP/J. K. Elbaum 1

Air Force Office of Scientifc Research
Propulsion Research Division
USAF
Washington, D. C. 20525
Attn: M. Slawsky 1

Army Materials Research Agency
Watertown Arsenal
Watertown, Massachusetts 02172
Attn: S. V. Arnold, Director 1

Department of the Army
Frankford Arsenal
Philadelphia, Pennsylvania 19137
Attn: MRL/H. Rosenthal 1

Department of the Navy
NASA Air-5203
Washington, D. C. 20360
Attn: P. Goodwin 1

Department of the Navy
ONR, Code 439
Washington, D. C. 20525
Attn: R. Roberts 1

Department of the Navy
Naval Ship R/D Center
Annapolis, Maryland 21402
Attn: G. J. Danek 1

U. S. Atomic Energy Commission
Washington, D. C. 20545
Attn: Technical Reports
Library 1
J. Simmons 1

Oak Ridge National Laboratory
Oak Ridge, Tennessee 37830
Attn: Technical Reports
Library 1

Defense Documentation Center/DDC
Cameron Station
5010 Duke Street
Alexandria, Virginia 22314 1

Aerojet-General Corporation
Azusa, California 91702
Attn: I. Petker 1

Aerospace Corporation
Reports Acquisition
P. O. Box 95085
Los Angeles, California 90045 1

Allegheny Ludlum Steel Corporation
Research Center
Brackenridge, Pennsylvania 15014
Attn: R. A. Lula 1

American Society for Metals
Metals Park
Novelty, Ohio 44073
Attn: T. Lyman 1

Amsted Research Laboratories
P. O. Box 567
Bensenville, Illinois 60106
Attn: E. J. Zickefoose 1

AVCO Lycoming Division
505 South Main Street
Stratford, Connecticut 06497
Attn: W. H. Freeman 1

AVCO Space Systems Division
Lowell Industrial Park
Lowell, Massachusetts 01851
Attn: Library 1

Battelle Memorial Institute
505 King Avenue
Columbus, Ohio 43201
Attn: R. I. Jaffee 1
B. Wilcox 1
Cobalt Info. Center 1
S. J. Paprocki 1

The Bendix Corporation
Research Laboratories Division
Southfield, Michigan 48075
Attn: Library 1

Boeing Company
P. O. Box 733
Renton, Washington 98055
Attn: W. E. Binz, SST Unit
Chief 1

Cabot Corporation
Stellite Division
1020 West Park Avenue
Kokomo, Indiana 46901
Attn: Library 1

Case Institute of Technology
University Circle
Cleveland, Ohio 44106
Attn: Department of Metallurgy 1

Climax Molybdenum Company
1600 Huron Parkway
Ann Arbor, Michigan 48106
Attn: M. Semchyshen 1

Curtiss-Wright Corporation
760 Northland Avenue
Buffalo, New York 14215
Attn: C. Wagner 1

Denver Research Institute
University Park
Denver, Colorado 80210
Attn: Library 1

Denver University
Metallurgy Department
Denver, Colorado 80210
Attn: J. B. Newkirk 1

Douglas Aircraft Company (MSFD)
3000 Ocean Park Boulevard
Santa Monica, California 90406
Attn: Library 1

Falconbridge Nickel Mines, Ltd.
7 King Street, East
Toronto, Ontario, Canada
Attn: L. G. Bonar 1

Federal Mogul Corporation
Research and Development Center
Ann Arbor, Michigan 48106
Attn: J. G. LeBrasse 1

Firth Sterling, Incorporated
Powders Metals Research
P. O. Box 71
Pittsburgh, Pennsylvania 15230 1

Ford Motor Company
Materials Development Department
20000 Rotunda Drive
P. O. Box 2053
Dearborn, Michigan 48123
Attn: Y. P. Telang 1

Fordon McKay Laboratory
6 Oxford Street
Cambridge, Massachusetts 02138
Attn: M. Ashby 1

Garrett-Air Research
Phoenix, Arizona 85034
Attn: Supv. Materials Engineering, Department 93393 1

General Electric Company
Advanced Technology Laboratory
Schenectady, New York 12305
Attn: Library 1

General Electric Company
Materials and Processes Laboratory
Schenectady, New York 12305
Attn: C. T. Sims 1

General Electric Company
Materials Development Laboratory Operations
Advance Engine and Technical Department
Cincinnati, Ohio 45215
Attn: L. P. Jahnke 1
R. E. Allen 1

General Motors Corporation
Allison Division
Indianapolis, Indiana 46206
Attn: K. K. Hanink, Materials Laboratory 1

Homogeneous Metals, Incorporated
West Canada Boulevard
Herkimer, New York 13350
Attn: R. J. Nylen 1

IIT Research Institute
10 West 35th Street
Chicago, Illinois 60616
Attn: N. M. Parikh 1

Industrial Materials Technology
127 Smith Place
West Cambridge Industrial Park
Cambridge, Massachusetts 02138
Attn: R. Widmer 1

International Nickel Company
67 Wall Street
New York, New York 10005
Attn: R. R. Dewitt 1

International Nickel Company
P. D. Merica Research Laboratory
Sterling Forest
Stuffern, New York 10901
Attn: F. Decker 1

Ladish Company
Government Relations Division
Cudahy, Wisconsin 53110
Attn: C. Burley, Jr. 1

Latrobe Steel Company
Latrobe, Pennsylvania 15650
Attn: E. E. Reynolds 1

Lockheed-Georgia Company
Research Laboratory
Marietta, Georgia 30060
Attn: W. S. Cremens 1

Lockheed Palo Alto Research Laboratories
Materials and Science Laboratory, 52-30
3251 Hanover Street
Palo Alto, California 94304
Attn: Technical Information Center 1

Martin Metals
250 North 12th Street
Wheeling, Illinois 60090
Attn: C. H. Lund 1

McDonnel-Douglas Corporation
3000 Ocean Park Boulevard
Santa Monica, California 90406
Attn: R. Johnson 1

McDonnel-Douglas Corporation
P. O. Box 516
St. Louis, Missouri 63166
Attn: R. E. Jackson 1

Michigan Technical University
Department of Metallurgical Engineering
Houghton, Michigan 49931
Attn: R. W. Guard 1

Micromet Laboratories
202 South Street
West Lafayette, Indiana 47906
Attn: J. F. Radavich 1

North American Rockwell Corporation
Rocketdyne Division
6633 Canoga Avenue
Canoga Park, California 91304
Attn: E. D. Weisert 1

North Star Research and Development Institute
3100 Thirty-Eight Avenue South
Minneapolis, Minnesota 55406
Attn: J. W. Clegg 1

Ohio State University
Department of Metallurgical Engineering
Columbus, Ohio 43210
Attn: R. A. Rapp 1

Nuclear Materials Company
West Concord, Massachusetts 01781
Attn: Library 1

Philco-Ford Corporation
Ford Road
Newport Beach, California 92663
Attn: R. A. Harlow 1

Polymet Corporation
11 West Sharon Road
Cincinnati, Ohio 45346
Attn: G. J. Wile 1

Reactive Metals, Incorporated
100 Warren Avenue
Niles, Ohio 44446
Attn: H. D. Kessler 1

Solar Division
International Harvester Corporation
San Diego, California 92112
Attn: J. V. Long, Director of Research 1

Special Metals Corporation
New Hartford, New York 13413
Attn: W. J. Boesch 1

Stanford Research Institute
Menlo Park, California 94025
Attn: E. S. Wright 1

Stanford University
Department of Materials Science
Palo Alto, California 94305
Attn: O. Sherby 1

Sylvania Electric Products,
Incorporated
Chemical and Metallurgical Division
Towanda, Pennsylvania 18848
Attn: J. S. Smith 1

Tem-Pres Research, Incorporated
1401 South Atherton Street
State College, Pennsylvania 16801
Attn: R. I. Harker 1

TRW, Incorporated
Materials Technology
23555 Euclid Avenue
Cleveland, Ohio 44117
Attn: Library 1
E. A. Steigerwald 1

Union Carbide Corporation
Speedway Laboratories
P. O. Box 24184
Indianapolis, Indiana 46224
Attn: Technical Library 1

United Aircraft Corporation
400 Main Street
East Hartford, Connecticut 06108
Attn: Research Library 1
E. F. Bradley, Chief,
Materials Engineering 1

United Aircraft Corporation
Pratt and Whitney Aircraft
Advanced Materials R/D Laboratory
Middletown, Connecticut 06458
Attn: C. P. Sullivan 1

United Aircraft Corporation
Pratt and Whitney Aircraft Division
West Palm Beach, Florida 33402
Attn: Library 1

Universal-Cyclops Steel Corporation
Bridgeville, Pennsylvania 14017
Attn: C. P. Mueller 1

Westinghouse Electric Corporation
Steam Division
P. O. Box 9175
Lester, Pennsylvania 19113
Attn: F. J. Wall 1

Wyman-Gordon Company
North Grafton, Massachusetts 01436
Attn: W. H. Couts 1